Numerical high-resolution air-sea coupling over the Gulf of Lions during two tramontane/mistral events

Cindy Lebeaupin Brossier, Philippe Drobinski

Numerical high-resolution air-sea coupling over the Gulf of Lions during two tramontane/mistral events

C. Lebeaupin Brossier[1] and P. Drobinski[1]

Received 8 December 2008; revised 4 March 2009; accepted 23 March 2009; published 29 May 2009.

[1] The near-sea-surface meteorological conditions associated with strong wind events over the Mediterranean Sea constitute a strong forcing on the ocean mixed layer. The present study addresses the question of the sea surface scheme used in high-resolution and short-range atmospheric numerical modeling to represent the ocean mixed layer response under these severe mistral wind events in the Gulf of Lions area. Several slab ocean models have been used coupled with the Weather Research and Forecasting (WRF) model and applied on two mistral cases: (1) a slab model based on the transport divergence equation where the mixed layer evolution is only driven by the wind stress, (2) a slab model where the temperature is the only prognostic variable and evolves according to the net surface heat flux, and (3) a complete slab scheme from Price (1981). The coupled simulations are also compared to two basic simulations, one using a constant sea surface temperature (SST) field during all of the model integration and another using a 6-hourly update sea surface temperature reanalysis. In this study, we mainly focus on the slab model performances. We identify the processes involved in the ocean mixed layer response under strong wind situations, i.e., local and fast cooling and deepening. The feedbacks of an interactive ocean mixed layer on the atmospheric simulation are also investigated.

Citation: Lebeaupin Brossier, C., and P. Drobinski (2009), Numerical high-resolution air-sea coupling over the Gulf of Lions during two tramontane/mistral events, *J. Geophys. Res.*, *114*, D10110, doi:10.1029/2008JD011601.

1. Introduction

[2] The western Mediterranean basin is prone to severe weather events, such as strong winds or heavy precipitation situations, generally enhanced by the surrounding mountain ranges (Figure 1, top) and the intense air-sea exchanges. Air-sea interactions during heavy precipitation events over southeastern France have already been investigated by high-resolution and short-range numerical modeling [*Lebeaupin et al.*, 2006; *Lebeaupin Brossier et al.*, 2008, 2009]. The onshore low-level jet that frequently accompanies these rainfall events was evidenced as a key factor in the thermal exchanges that occur between the ocean mixed layer (OML) and the atmospheric boundary layer (ABL).

[3] The mistral is a northerly offshore wind that affects the southeastern France and the Gulf of Lions area. It is channeled and accelerated in the Rhône river valley between the surrounding mountains (Alps and Massif Central, Figure 1, bottom). It transports cold continental air over the Mediterranean Sea and induces both strong momentum and heat exchanges at the air-sea interface [*Flamant*, 2003], sea surface cooling and sometimes coastal upwellings [*Millot*, 1979; *Estournel et al.*, 2003]. This strong local wind is also known to be the main ingredient involved in ocean convection and deep water formation in the Gulf of Lions [*Li et al.*, 2006]. High-resolution atmospheric numerical models have already shown their good ability to simulate the spatial complexity of these strong wind events and their unsteadiness [*Drobinski et al.*, 2005; *Bastin et al.*, 2006; *Guénard et al.*, 2006; *Salameh et al.*, 2007]. The next step for understanding the ocean-atmosphere interactions during mistral events can be achieved by the use of a high-resolution coupled model. In rare studies, the full two way coupling at high-resolution has been investigated in extreme weather conditions like in bora situations over the Adriatic Sea [*Pullen et al.*, 2003, 2006, 2007] where the bora is a strong offshore wind similar to the mistral. *Pullen et al.* [2006] found that the Adriatic Sea feedback, taken into account in a two-way coupling, significantly improved their model performances in bora situations. In the two-way coupling, they found a reduction of the mean bias of wind speed and of the sea surface temperature (SST) against observations (buoys or satellite data) compared to one-way coupling. In heavy precipitating situations, *Lebeaupin Brossier et al.* [2009] found that the two-way coupling tends to limit the two boundary layers response, with less precipitation amounts and smaller SST cooling compared to one-way simulation.

[4] In order to evaluate the strong air-sea exchanges that occur during mistral events between the ABL and OML, an alternate way to full two-way tridimensional coupling development is using a slab ocean scheme. We examined here the sensitivity of coupled high-resolution short-range simulations to various slab ocean model configurations. This simple ocean scheme has already been coupled to atmospheric

[1]Laboratoire de Météorologie Dynamique, Institut Pierre Simon Laplace, Ecole Polytechnique, ENS, UPMC, CNRS, Palaiseau, France.

0148-0227/09/2008JD011601

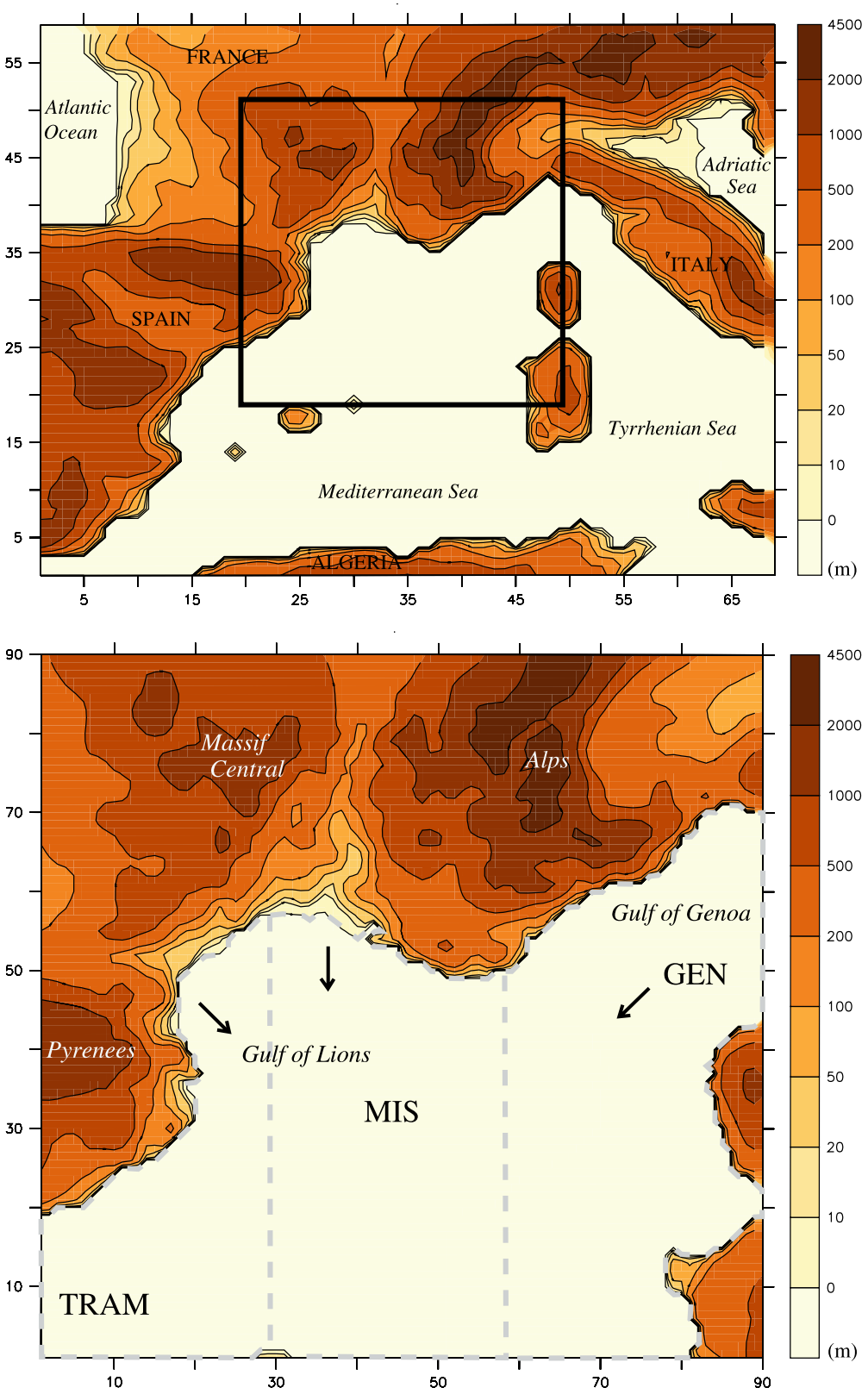

Figure 1. Domains of simulation at (top) 21-km and (bottom) 7-km resolution (topography in meters). The X,Y labels indicate the grid-point numbers. In the top panel the inner domain borders are 36.2°N/47.2°N and 3.2°W/14.2°E. In the bottom panel the GEN, MIS, and TRAM labels indicate the three sea subdomains characterized by various wind regimes: Ligurian outflow over the Gulf of Genoa and mistral and tramontane over the Gulf of Lions, respectively.

Table 1. Numerical Experiments

Experiment	Description	Parameters
REF	constant SST	
NCEPUP	SST update every 6h from reanalysis	
Ocean schemes		
ORIGOML	original WRF slab scheme; (Davis and Holland, presented paper, 2007); processes modeled: coriolis, entrainment, and wind stress	$h(0) = 50$ m, $\gamma = 0.14$ K/m
SLABOML	slab thermal scheme; [*Gaspar*, 1988]; processes modeled: surface heat fluxes	$h = h(0) = 50$ m
COMPOML	complete slab scheme; processes modeled: coriolis, entrainment, wind stress, and surface heat fluxes	$h(0) = 50$ m, $\gamma = 0.14$ K/m

models in order to estimate the air-sea exchanges in several studies [*Gaspar*, 1988; *Schade and Emanuel*, 1999; *Drévillon et al.*, 2003; *Lau and Nath*, 2006; G. Samson et al., Numerical investigation of an oceanic resonant regime induced by hurricane winds, submitted to *Ocean Dynamics*, 2009]. This sea scheme is here applied in simulations of two past intense mistral events: the unsteady 23–26 March 1998 event with mistral maximum intensity of 15–20 m s^{-1} lasting less than one day and the more stationary 5–9 November 1999 cases with maximum intensity of 20–30 m s^{-1} lasting more than 2 days. The slab ocean model available in the WRF model is based on the wind-mixed layer model from *Pollard et al.* [1973] including the Coriolis force. It was coupled to the WRF model in the framework of C. Davis and G. Holland's study for application on tropical cyclones (Realistic simulations of intense hurricanes with the NCEP/NCAR WRF modeling system, paper presented at 10th Workshop on Wave Hindcasting and Forecasting and Coastal Hazard Symposium, U.S. Army Engineer Research and Development Center, Oahu, Hawaii, 2007). We take benefit of this coupling available in the WRF model to evaluate the impact of such a slab ocean model in other high-wind situations at midlatitudes. In addition, we investigate the possibility of improving such a slab model. In particular, we made modifications in the original slab ocean scheme available in order to take the surface heat budget into account. Other numerical schemes as experienced by *Kara et al.* [2008] study could be considered, but we restricted here to the three slab model configurations presented in the experimental design (section 2).

[5] The main objectives of this study are: (1) to evaluate the fine scale OML evolution in terms of depth and SST under mistral; (2) to identify the main processes involved in the ocean response (entrainment, advection, and surface exchanges) to the mistral by comparing the different slab ocean scheme responses; and (3) to estimate the feedbacks of an interactive OML on the atmospheric simulation by examining the sensitivity of the surface heat fluxes, temperature, humidity, and pressure fields to the different slab ocean schemes. The experimental design is presented in the following section. A simulations results intercomparison is detailed in section 3. A conclusion follows in section 4.

2. Experimental Design

2.1. Numerical Atmospheric Model

[6] Numerical experiments have been performed with version 3.0 of the Weather Research and Forecasting (WRF) model of the National Center for Atmospheric Research (NCAR) [*Skamarock et al.*, 2008]. Two interactive nested domains are used with mesh grids of 21 km and 7 km horizontal resolution, respectively. The outer domain (domain 1) covers the western Mediterranean basin and the inner domain (domain 2) is centered over the Gulf of Lions (Figure 1). In the vertical, 28 sigma levels are used [*Gal-Chen and Sommerville*, 1975].

[7] Initial and lateral conditions are given by the National Centers for Environmental Prediction (NCEP) reanalysis (NNRP or R1 products) [*Kalnay et al.*, 1996] with 2.5° × 2.5° horizontal resolution available every 6 h and for 28 vertical levels. Over the sea, the NCEP reanalysis tridimensional variational data assimilation system [*Kalnay et al.*, 1996] uses buoy and ship data of surface pressure, surface temperature, air temperature, horizontal wind, and specific humidity and also vertical temperature soundings from the National Oceanic and Atmospheric Administration (NOAA) polar orbiters. For the SST, the weekly Reynolds SST fields are used as background. Because of the NCEP reanalysis's coarse resolution, the SST fields are relatively smoothed. They both show a northwest-southeast gradient (with a difference of nearly 5°C between the French coasts and the Balearic Islands). The SST mean values over domain 2 are 13.38°C on 23 March 1998 and 19.56°C on 5 November 1999. If the NCEP SST field used initially for the mis1 case is consistent with the monthly climatology from *Smith and Reynolds* [2003], on 5 November 1999, NCEP reanalysis displays a SST warmer by nearly 2°C over the region compared to the climatology (not shown). Indeed, for the mis1 case in March 1998, the SST is cold because of the ocean heat loss during the winter. The thermal contrast at the air-sea interface is thus small, producing moderate heat exchanges, even under strong winds. On the contrary, for the mis2 case, the SST is still warm because of the heat gain during the preceding summer and fall. This enhances the heat exchanges across the air-sea interface under strong winds.

[8] For the two interactive models, the microphysical scheme is WRF Single-Moment 3-class (simple ice-WSM3) scheme [*Hong et al.*, 2004]. The convection is parameterized by the new Kain-Fritsch convective scheme [*Kain*, 2004]. The turbulence scheme is the Yonsei University (YSU) planetary boundary layer (PBL) scheme [*Noh et al.*, 2003]. The radiative scheme is the Rapid Radiative Transfer Model (RRTM) [*Mlawer et al.*, 1997] for the longwave flux and the *Dudhia* [1989] parameterization for the shortwave (solar)

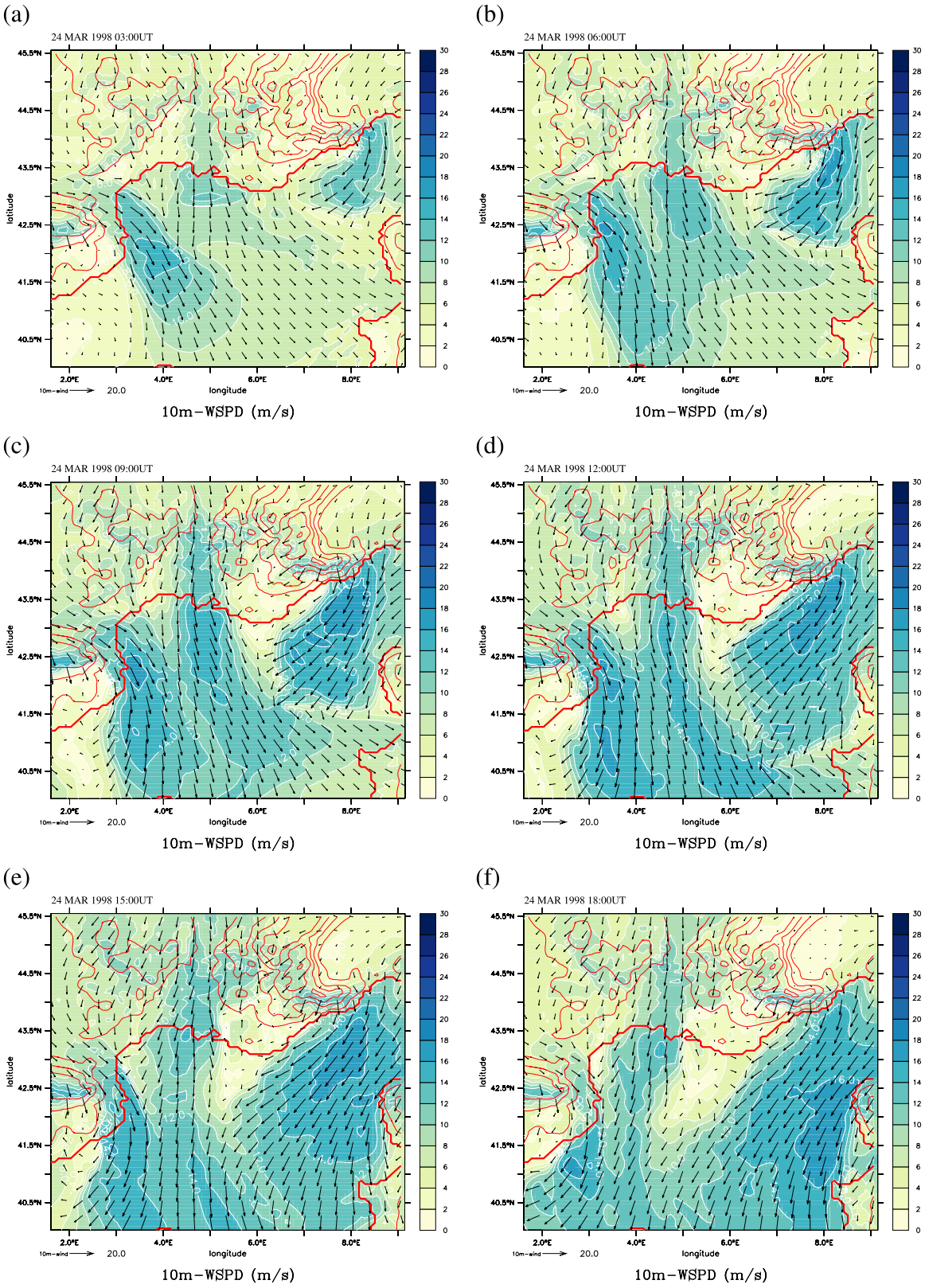

Figure 2. The 10-m wind speed (m s^{-1}) over domain 2 simulated by the REF experiment on 24 March 1998 at (a) 0300 UT, (b) 0600 UT, (c) 0900 UT, (d) 1200 UT, (e) 1500 UT, and (f) 1800 UT. Red lines delineate every 500 m topography height.

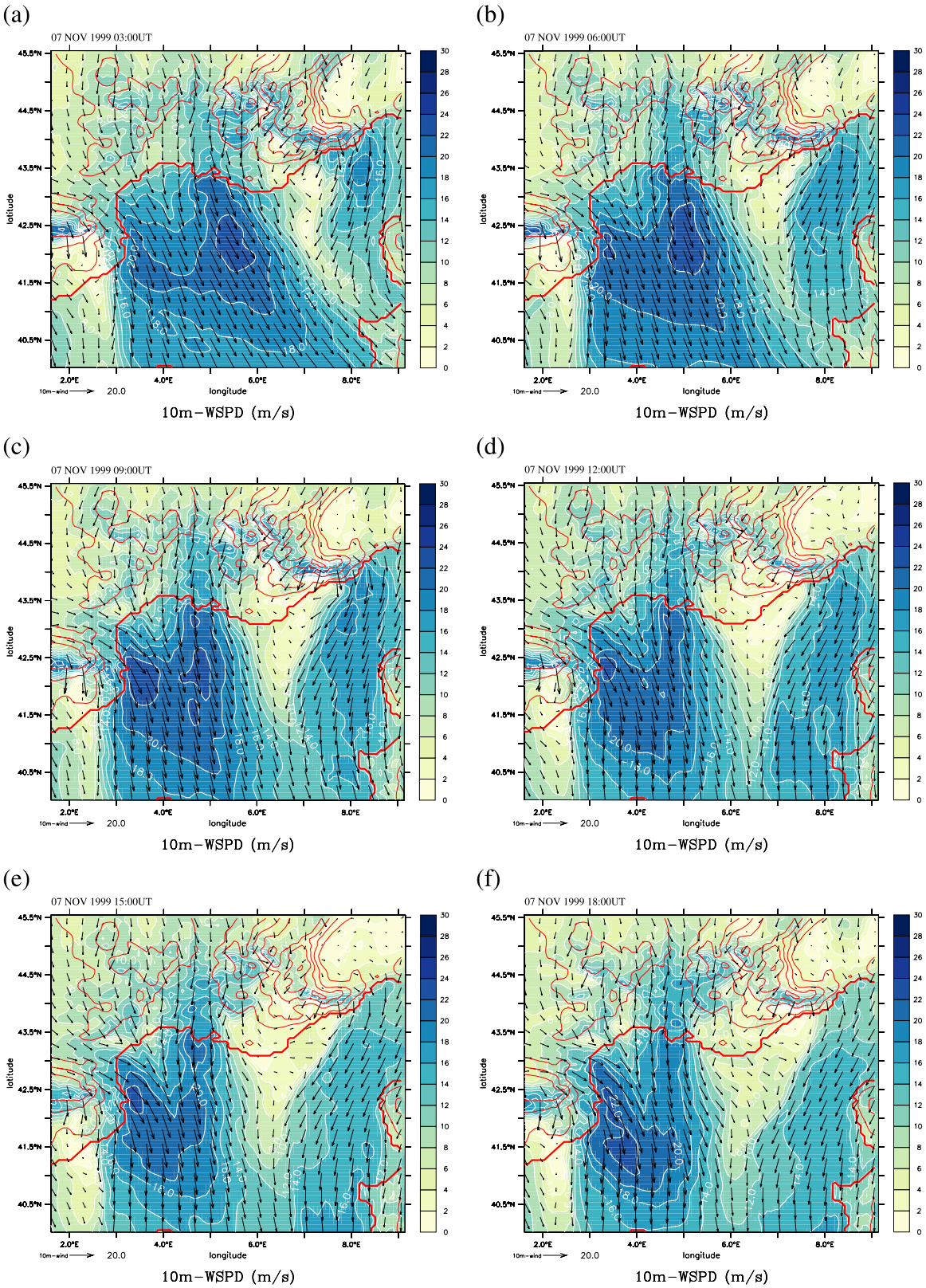

Figure 3. As in Figure 2 but simulated by the REF experiment for 7 November 1999 at (a) 0300 UT, (b) 0600 UT, (c) 0900 UT, (d) 1200 UT, (e) 1500 UT, and (f) 1800 UT.

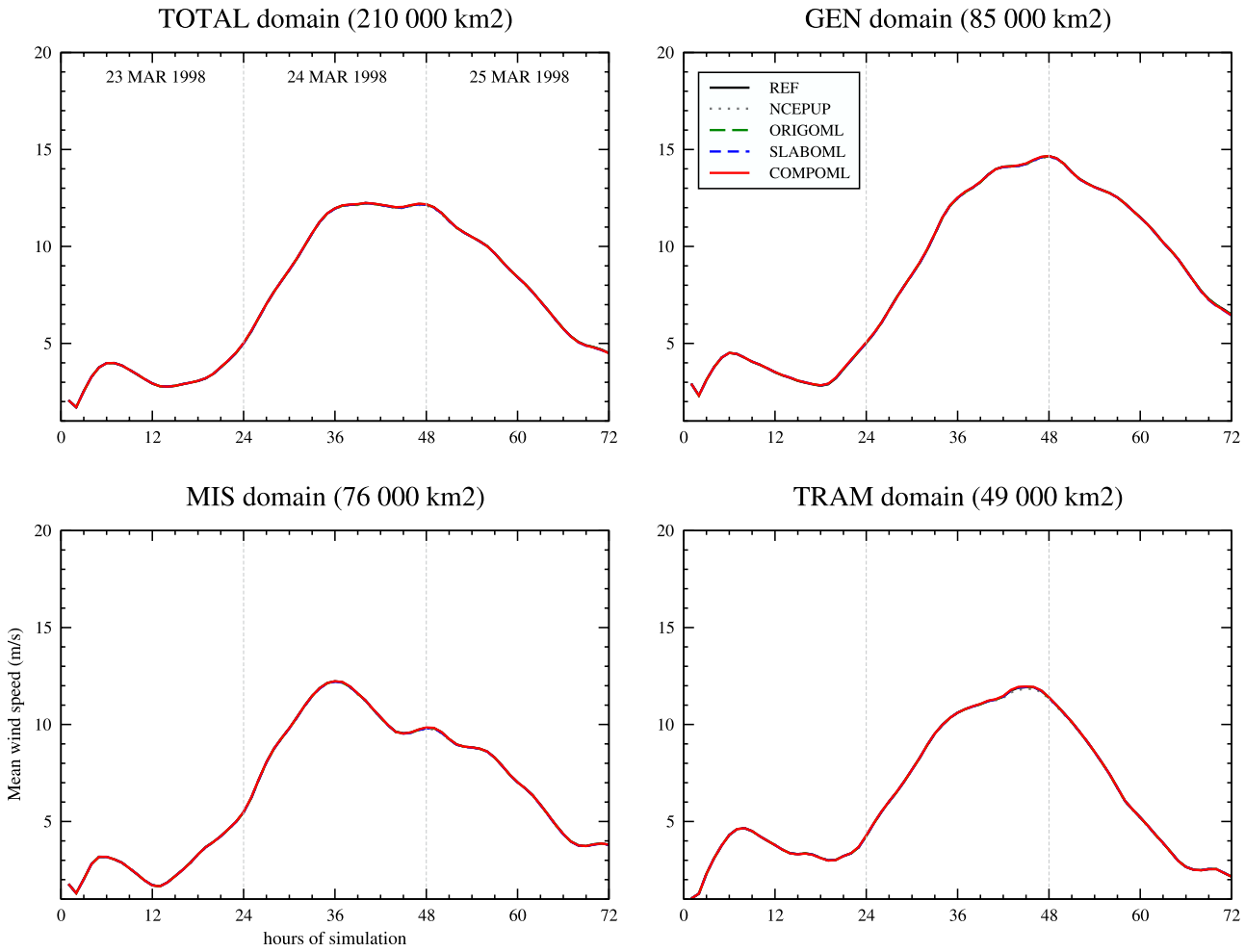

Figure 4. Temporal evolution of the mean 10-m wind speed (m s^{-1}) during the mis1 case simulations over the TOTAL Sea domain and the GEN, MIS, and TRAM sea domains (see Figure 1). Note that the time range is not the same as for mis2 case in Figure 6.

flux. The turbulent surface fluxes are computed with a parameterization based on the similarity theory [*Monin and Obukhov*, 1954]. For the land surface, the thermal diffusion scheme (slab scheme) is used. In this study, several options for the sea surface scheme were used (see the following subsection and Table 1).

2.2. Ocean Schemes

[9] Simulations begin 23 March 1998 at 0000 UT and 5 November 1999 at 0000 UT, and last 72 and 96 h, respectively. For each event, we produce the same set of numerical experiments summarized in Table 1.

[10] The reference experiments (REF) use the simplest configuration for the sea surface scheme, i.e., the initial SST from NCEP reanalysis valid for the simulation initial time (i.e., 23 March 1998 0000 UT and 5 November 1999 0000 UT) is kept constant during the simulation duration. In simulations called NCEPUP, the SST field is updated at the NCEP reanalysis availability frequency, i.e., every 6 h.

[11] In the slab scheme, an ocean mixed layer is represented as a layer of depth h_0 initially homogeneous over the whole basin with a temperature T_0 initially equal to the SST over its whole depth. The horizontal current in the OML $\vec{v_0}$ is initially zero. The OML is limited in depth by a strongly stratified thin layer called the upper thermocline and defined by a temperature gradient γ. Under the stratified layer, we assume the presence of a deep abyssal layer. In this scheme, the OML deepening is estimated from the transport divergence (equation (1)); the OML temperature is estimated from the heat balance (equation (2)) and the horizontal current from the momentum balance (equation (3)). Salt is not taken into account [*Pollard et al.*, 1973; *Price*, 1981],

$$\frac{\partial h}{\partial t} + \vec{\nabla}.(h\vec{v}) = w_e, \tag{1}$$

$$\frac{\partial T}{\partial t} + \vec{v}.\vec{\nabla}T = \frac{Q}{\rho_0 c_p h} + \frac{w_e(T - T_d)}{h}, \tag{2}$$

$$\frac{\partial \vec{v}}{\partial t} + (\vec{v}.\vec{\nabla})\vec{v} = -f\vec{k} \wedge \vec{v} - \frac{1}{\rho_0}\vec{\nabla}p + \frac{\vec{\tau}}{\rho_0 h} + \frac{w_e(\vec{v} - \vec{v_d})}{h}, \tag{3}$$

where $\vec{\nabla}$ is the horizontal gradient operator, $\vec{v}$ is the horizontal current in the OML, T is its temperature, and h is

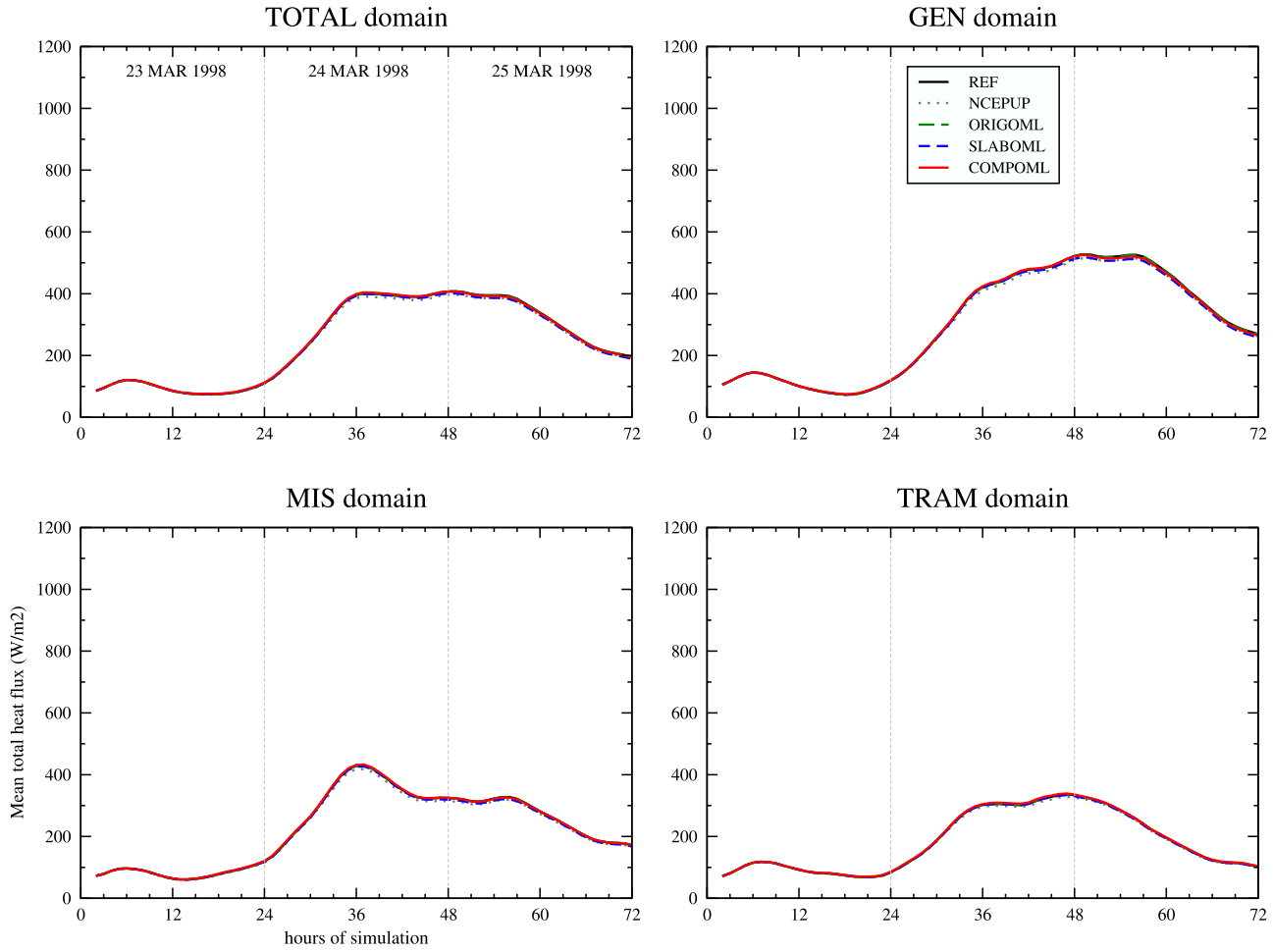

Figure 5. Temporal evolution of the mean total heat flux (H + LE W m^{-2}) during the mis1 case simulations over the TOTAL Sea domain and the GEN, MIS, and TRAM sea domains. Note that the time range is not the same as for mis2 case in Figure 7.

its depth. T_d and v_d are the temperature and current in the deepest layer: generally v_d is null and T_d is defined by the parameter $\frac{T-T_d}{h_0} = \gamma > 0$. Q is the net heat flux at the surface; $\vec{\tau}$ is the wind stress; f is the Coriolis parameter; ρ_0 and c_p are the density and the specific heat of sea water; and w_e is the vertical entrainment speed.

[12] The pressure gradient in the OML over an infinite depth layer can be expressed as

$$\vec{\nabla} p = g\left[h\vec{\nabla}\rho - \delta\rho\vec{\nabla}h\right], \tag{4}$$

where ρ is the OML water density, g is the gravity acceleration and $\delta\rho$ is the density difference between the OML and the deep abyssal layer.

[13] In ORIGOML simulations (Table 1), we use the coupled ocean model available in WRF (hereafter referred as the original model). It is based on the wind-mixed layer model of *Pollard et al.* [1973] and was coupled to WRF to study ocean feedbacks during hurricanes (Davis and Holland, presented paper, 2007). The *Pollard et al.* [1973] model assumes that the current and the OML depth h evolve according to the wind stress near the surface and the Coriolis force [*Ekman*, 1905].

[14] Ignoring horizontal advection, the time rate of change of the vertically averaged horizontal momentum of the upper ocean is given by

$$\frac{\partial hu}{\partial t} = fhv + \frac{\tau_x}{\rho_0} \tag{5}$$

$$\frac{\partial hv}{\partial t} = -fhu + \frac{\tau_y}{\rho_0}. \tag{6}$$

The temperature evolution is thus driven by the entrainment due to the OML deepening that brings colder water from the deepest layer into the OML and of the Ekman transport. The surface heat fluxes are neglected in this scheme (Q = 0). Indeed several studies showed that the surface heat fluxes are negligible by comparison to the heat loss through the OML base in tropical cyclones [*Bender et al.*, 1993; *Schade and Emanuel*, 1999; *Emanuel et al.*, 2004].

[15] In SLABOML simulations sea scheme (Table 1), the OML depth is kept constant during the simulation integration

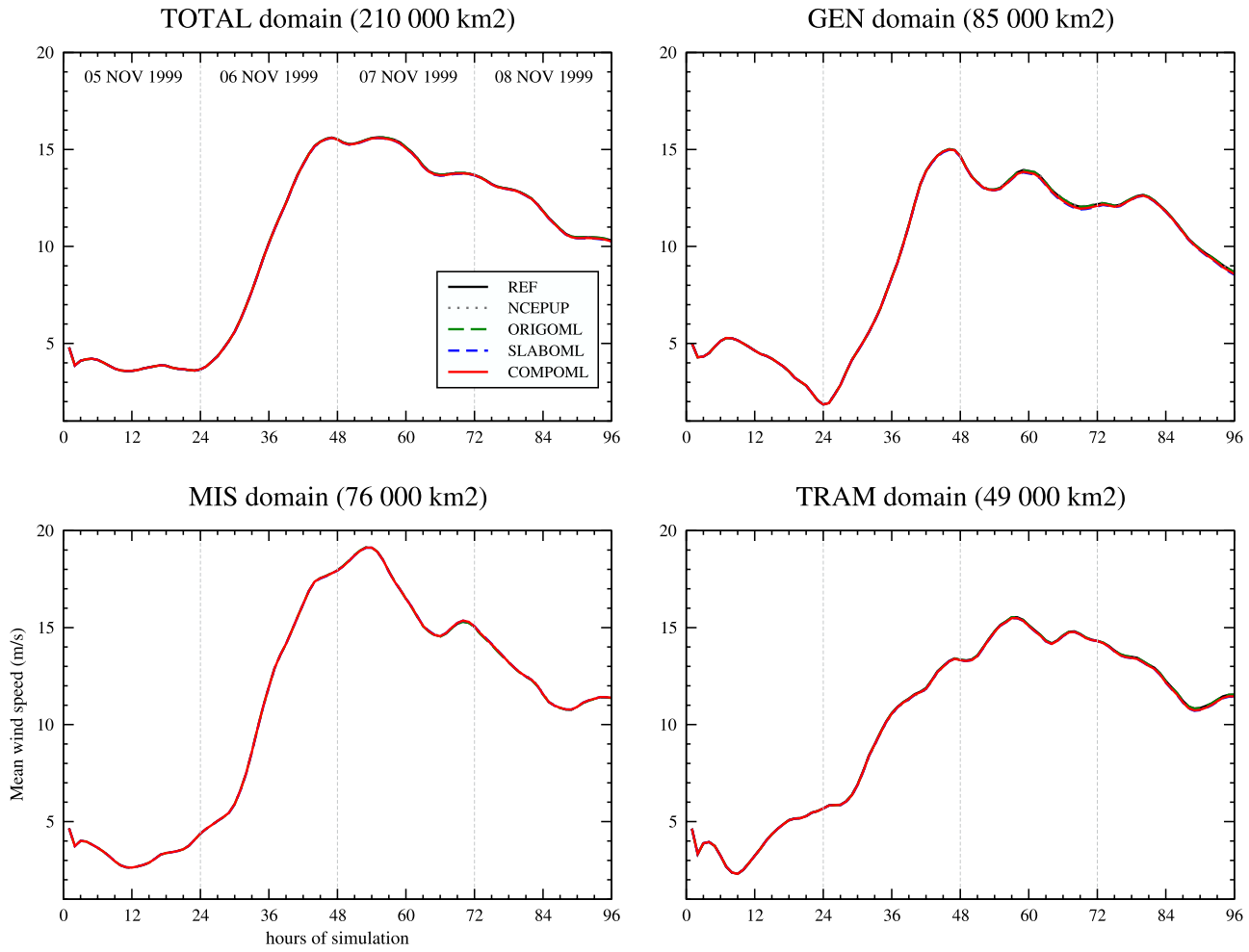

Figure 6. As in Figure 4 but during the mis2 case simulations. Note that the time range is not the same as for mis1 case in Figure 4.

(w_e = 0) and the currents are not taken into account. The temperature evolves only according to the net heat budget at the surface [*Gaspar*, 1988]. Finally, equation (2) reduces to

$$\frac{\partial T}{\partial t} = \frac{Q}{\rho c_p h} \tag{7}$$

$$Q = F_{sol} + F_{IR_{net}} - H - LE. \tag{8}$$

F_{sol} is the (downward) solar flux and $F_{IRnet} = F_{Irdown} - F_{IRup}$ is the net infrared flux. H and LE are the sensible and latent heat fluxes, respectively. This slab scheme applied to the high-resolution and short-range simulation of heavy precipitating events over the same area already showed strong SST tendencies in the Gulf of Lions, especially under onshore low-level wind [*Lebeaupin et al.*, 2006].

[16] In COMPOML simulations (Table 1), the full equation system (equations (1), (2) and (3)) is solved during the model integration in order to take into account the surface heat and momentum fluxes, the Coriolis force, the entrainment and the Ekman transport effects on the OML.

2.3. Simulated Meteorological Situations

[17] The development of the mistral is preconditioned by cyclogenesis over the Gulf of Genoa and the passage of a trough through France. When the synoptic northerly flow reaches the Alpine range, it experiences channeling in the Rhône valley. The flow is substantially accelerated, producing the mistral. The mistral occurs all year long but exhibits a seasonal variability either in speed and direction, or in its spatial distribution.

[18] In this study, we focus on two mistral events from 23 March 1998 0000 UT to 26 March 1998 0000 UT (72 h) hereafter referred as "mis1" and from 5 November 1999 0000 UT to 9 November 1999 0000 UT (96 h) referred as "mis2."

2.3.1. The 23–26 March 1998 "mis1" Event

[19] Between the 23 and 26 March 1998, as an upper-level trough associated with a cold front progresses toward the Alps, a shallow vortex moves over the Tyrrhenian Sea. The low over the Tyrrhenian deepens while moving to the southeast between 0600 UT and 2100 UT 24 March) and reaches Sicily on 25 March 1998 at 0600 UT. It induces a very nonstationary wind regime over the Gulf of Lions at low levels characterized by three converging flows (Figure 2): a northwestern flow (tramontane), Northerly winds in the

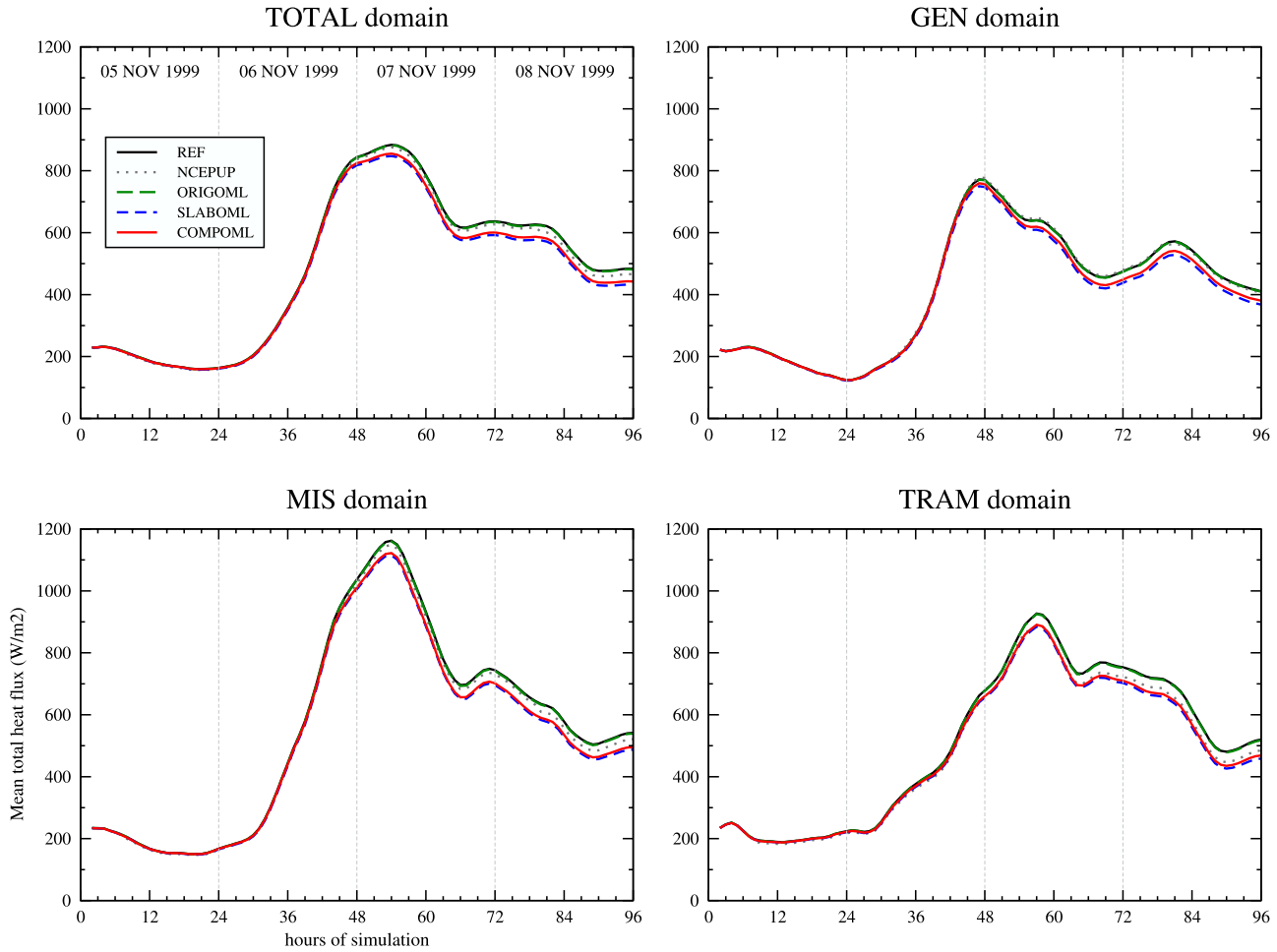

Figure 7. As in Figure 5 but during the mis2 case simulations. Note that the time range is not the same as for mis1 case in Figure 5.

Rhône valley (mistral) and a northeastern flow in the Gulf of Genoa (Ligurian outflow). In the morning of 24 March 1998, the tramontane prevails and the mistral extends all the way to Southern Corsica, wrapping around the depression. A weak Ligurian outflow is observed over the Gulf of Genoa. As the low deepens, the prevailing wind regime shifts to a well-established mistral which peaks around 1200 UT on 24 March and is observed to reach southern Sardinia. At this time the Ligurian outflow has become stronger. In the afternoon (1500 UT), the mistral is progressively disrupted by the strengthening Ligurian outflow in response to the deepening low and the channeling induced by the presence of the Alpine ranges. In the evening, the mistral is again well established as the depression continues to deepen (2100 UT) but moves to the southeast, reducing the influence of the Ligurian outflow. During this period, the tramontane appears to be much more steady than the mistral and less disrupted by the Ligurian outflow. Maximum low-level winds reach about 20 m s^{-1} over the Gulf of Lions and 30 m s^{-1} over the Ligurian Sea on 24 March 1998. The mistral transports a cold air mass containing continental and urban aerosols to North Africa, as a relative warmer air mass is isolated over Sea to the west of Sardinia [*Salameh et al.*, 2007]. The cold air outbreak over the Gulf of Lions ends in the morning of 25 March and anticyclonic conditions then prevail. The reader is referred to *Flamant* [2003] and *Salameh et al.* [2007] for a fully detailed description of the synoptic and mesoscale conditions.

2.3.2. The 5–9 November 1999 "mis2" Event

[20] A mistral event occurs between 5 and 9 November 1999 (Figure 3): it is characterized by the passage of a cut-off low over the North Sea associated with a marked upper westerly flow blowing at 40 m s^{-1} at 500 hPa at 0000 UT on 6 November. A marked upper northwesterly flow behind the cold front is associated with the cyclone. After 0000 UT on 7 November, the Genoa cyclogenesis is triggered in the lee of the Alps. The presence of the Azores ridge over western France maintains a moderate north westerly geostrophic wind at 500 hPa (around 20 m s^{-1}). At 0000 UT on 8 November, the Genoa cyclone moves southeastward while the Azores ridge moves northeastward. The 500-hPa geostrophic winds veer southward over the northwestern Mediterranean until 0000 UT on 9 November. Near the surface, the mistral onset occurs at around 0000 UT on 6 November. The mistral peaks at 0000 UT on 7 November with intensities reaching 20–30 m s^{-1} and veers progressively from the northwest to the north. After 0000 UT, the mistral becomes more steady. The mistral strength slowly decreases until its

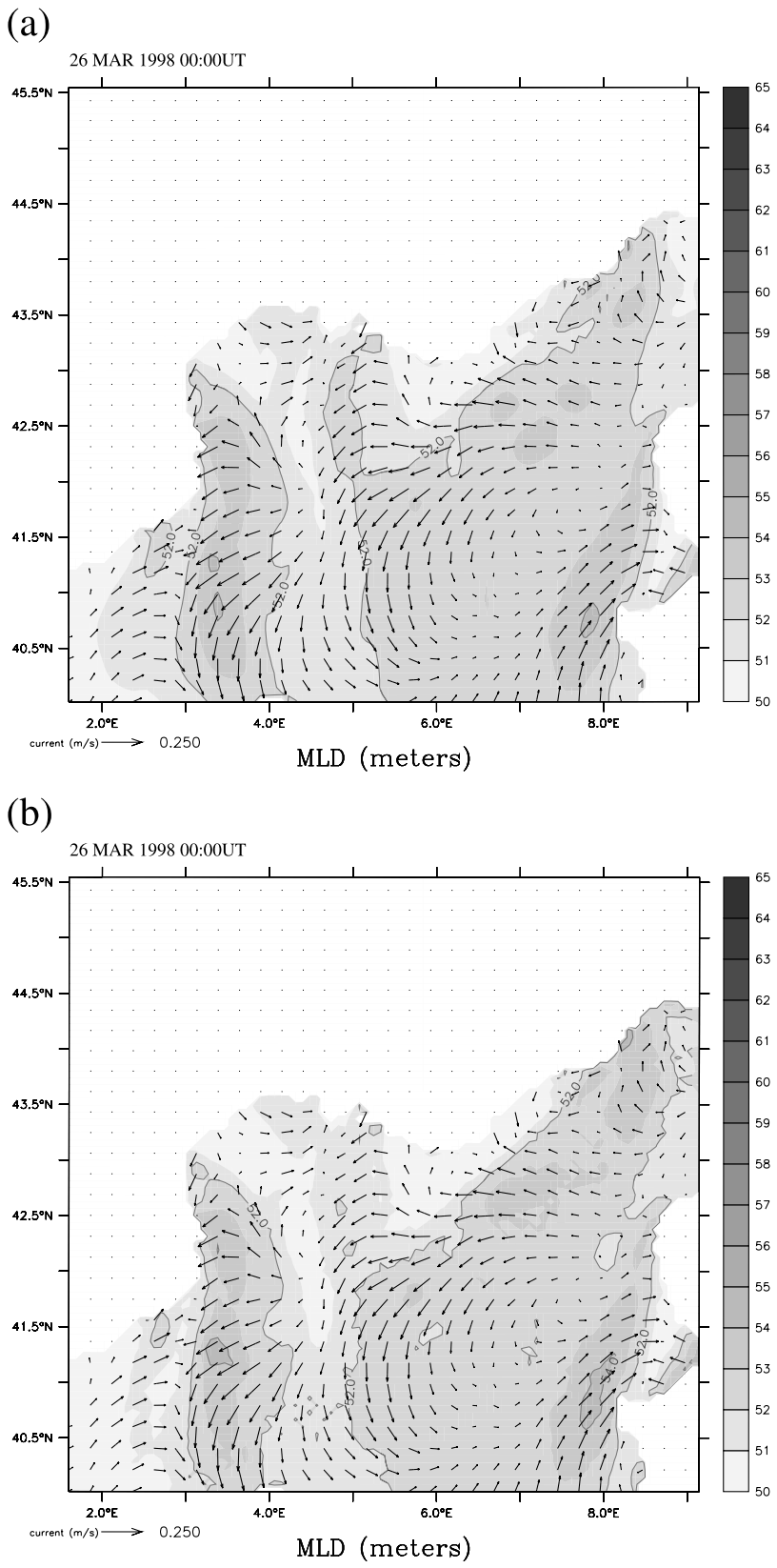

Figure 8. Ocean mixed layer depth (meters) and current (m s^{-1}) simulated by (a) ORIGOML and (b) COMPOML on 26 March 1998 0000 UT over domain 2. Initial OML depth value is 50 m over all the basin.

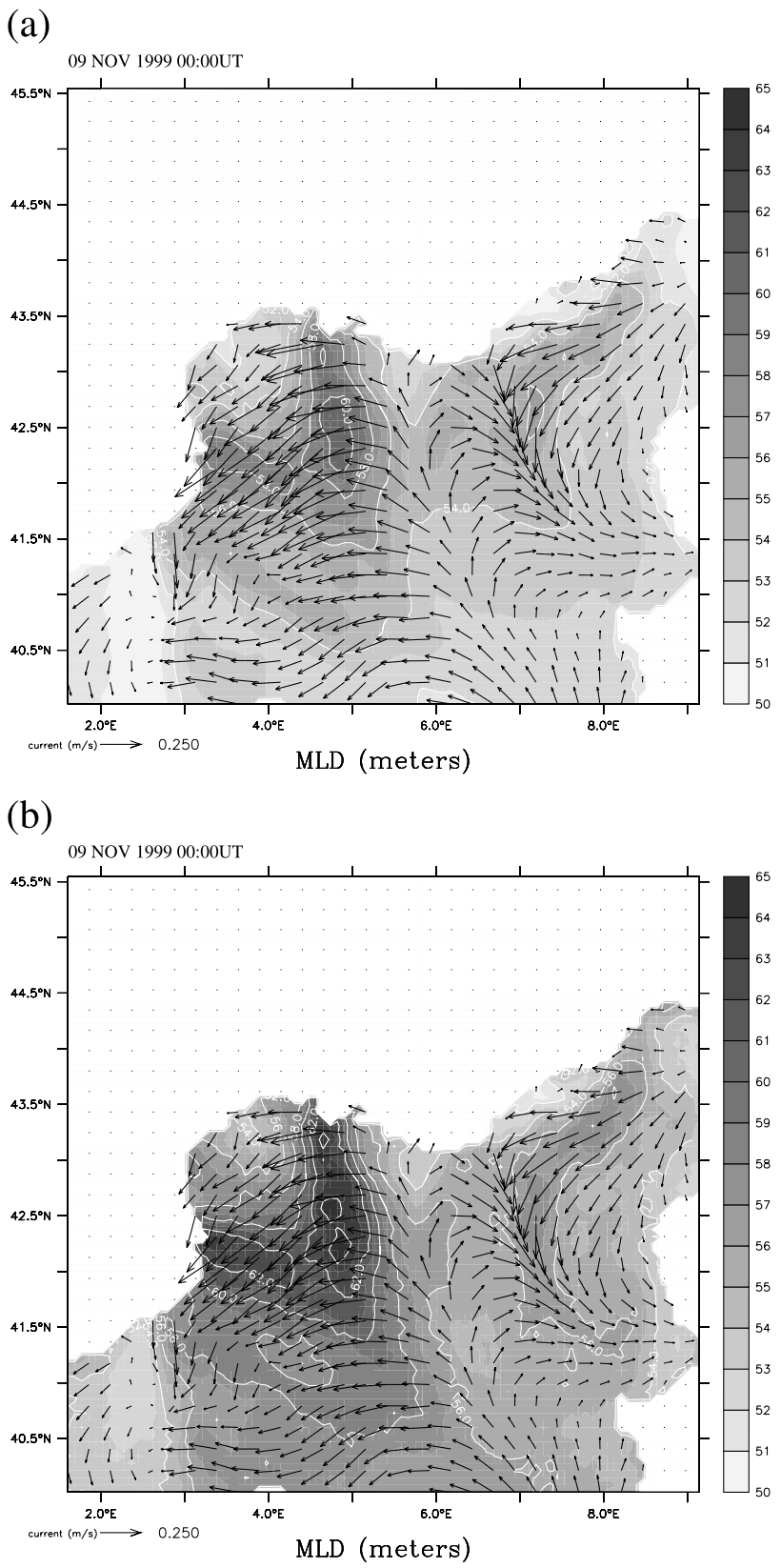

Figure 9. As in Figure 8 but simulated on 9 November 1999 0000 UT over domain 2 by (a) ORIGOML and (b) COMPOML.

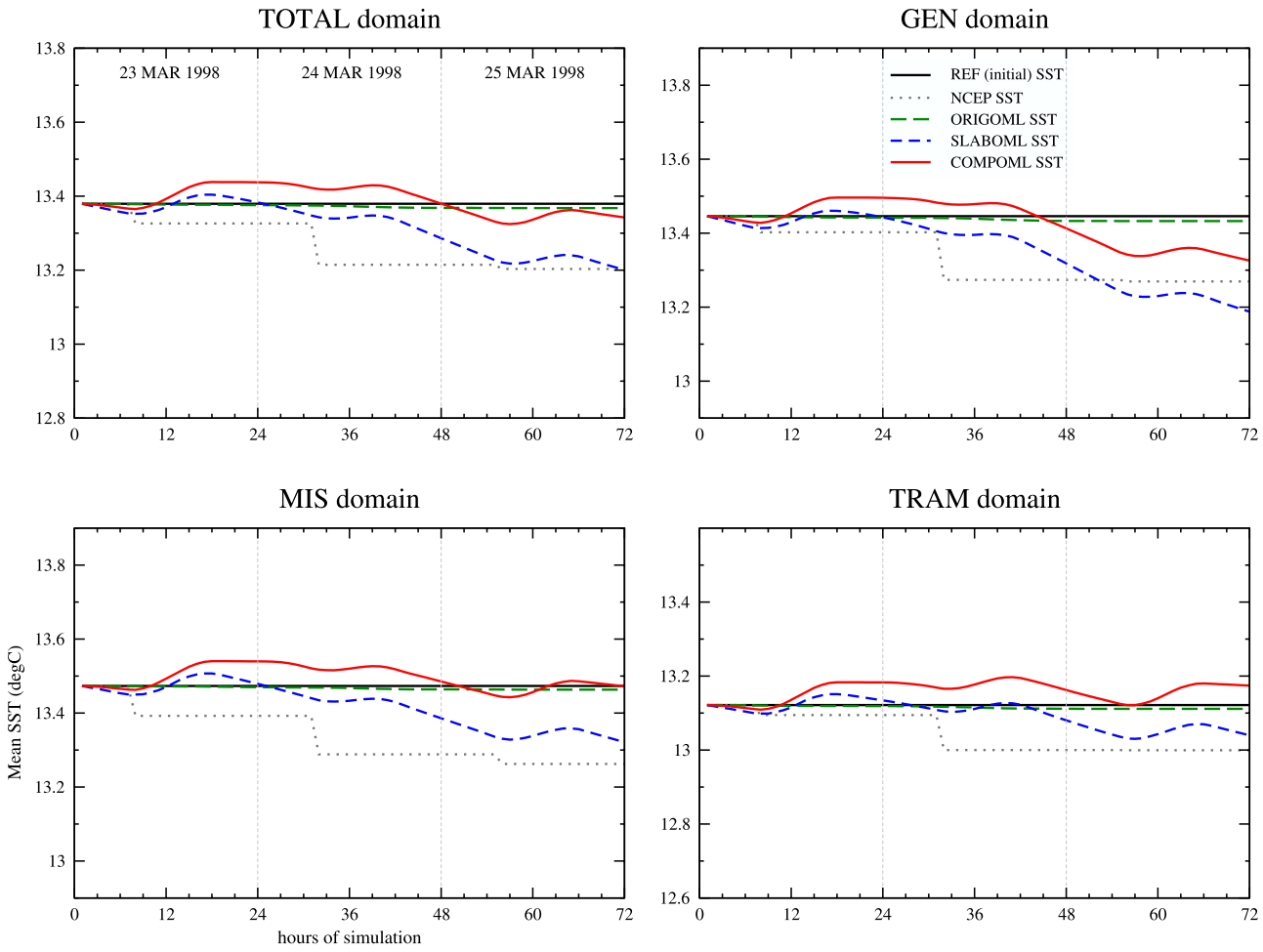

Figure 10. Temporal evolution of the mean SST (°C) during the mis1 case simulations over the TOTAL Sea domain and the GEN, MIS, and TRAM sea domains. Note that the time range is not the same as for mis2 case in Figure 12.

breakdown at 0000 UT on 9 November [*Guénard et al.*, 2006].

3. Simulations Intercomparison

3.1. Reference Experiments

[21] The reference simulation of the mis1 case succeeds in representing the upper-level dynamics. In particular, WRF captures the upper-level trough motion southward over the Tyrrhenian Sea during the afternoon of 24 March 1998 (not shown) and simulates accurately the strong low-level wind event in the Gulf of Lions (less than 2 m s^{-1} difference on average) with the distinct mistral and tramontane flows and the Ligurian outflow in the Gulf of Genoa. Figure 2 displays the evolution of the 10-m wind field over domain 2 on 24 March 1998 and Figure 4 plots the evolution of the 10-m wind speed averaged over domain 2 and the three subdomains shown in Figure 1. The strongest winds are simulated in the GEN domain during the night between 24 and 25 March 1998. The mistral intensity peak occurs on 24 March around 1200 UT and lasts only a few hours (Figures 2d and 4). It also corresponds to a peak in the energy amount transferred from the OML to the ABL as evidenced in Figure 5. The total turbulent heat flux ($H+LE$) exceeds 350 W m^{-2} on 24 March between 0900 UT and 1500 UT over the MIS subdomain. The high-resolution orography of domain 2 around the Gulf of Lions (in particular the Alps, Massif Central and Pyrénées, see Figure 1) allows the representation of the channeling process and the accurate simulation of the low-level wind field. WRF also succeeds in representing the unsteadiness of the mistral due to the Ligurian outflow as it was observed during the mis1 event (see section 2). The maximum 10-m wind speed is 18 m s^{-1} for the Ligurian outflow during the afternoon of 24 March. The 10-m wind field is also characterized by an area of relative weak wind located in the lee of the Alps (Figure 2).

[22] The reference experiment for the mis2 event also succeeds in correctly representing the upper level atmospheric dynamics with the Genoa cyclogenesis that slowly moves southeastward from the lee of the Alps to the Tyrrhenian Sea (not shown). At lower levels, the model simulates the mistral event (Figure 3), with a maximum mistral intensity between 20 and 25 m s^{-1} the morning of 7 November 1999 (against 14 m s^{-1} for the mis1 case reference; Figures 2 and 3). The mistral is also more steady compared to the mis1 case reference, with an average value of 15m s^{-1} of the 10-m wind speed over the MIS domain

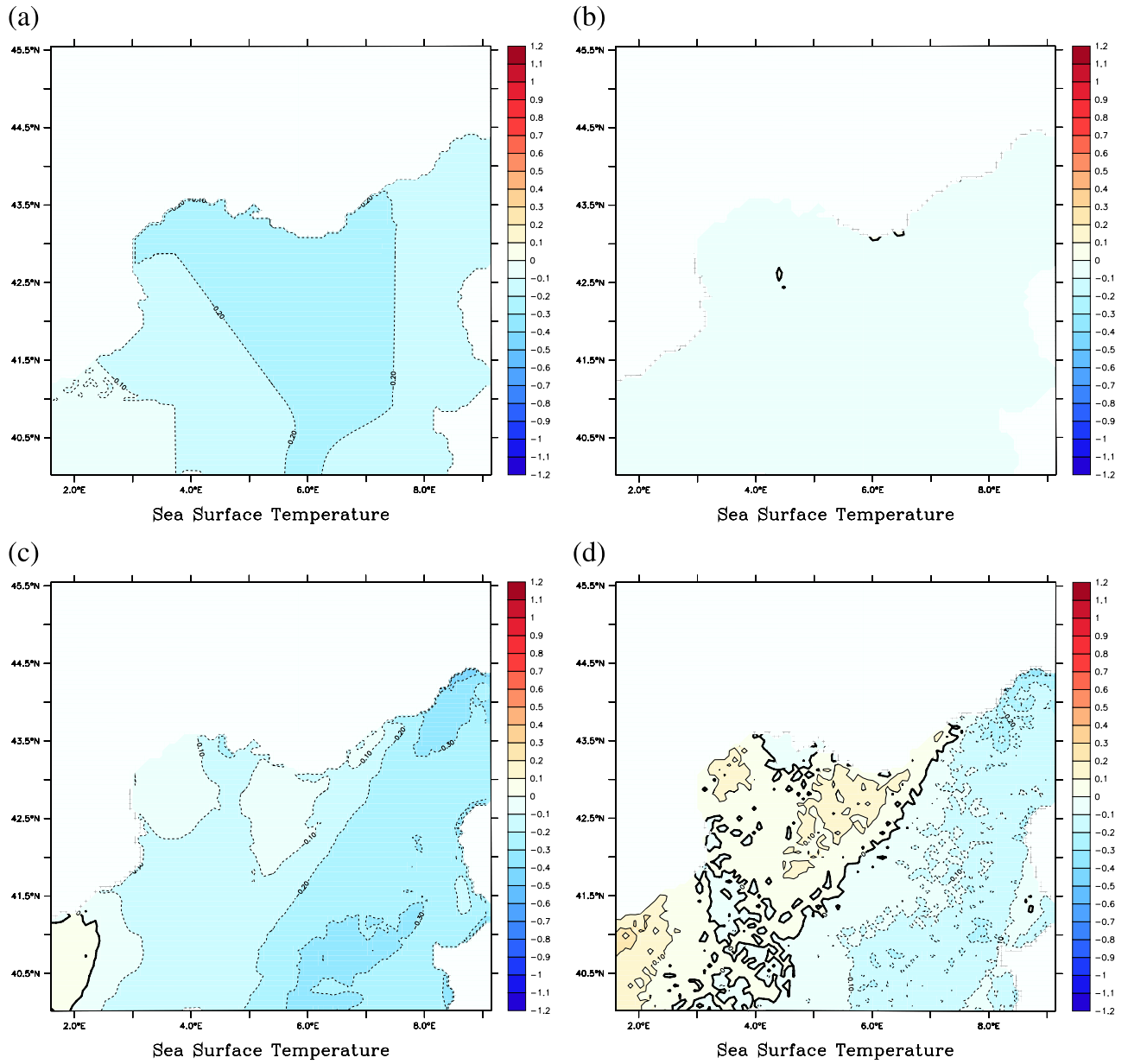

Figure 11. The mis1 case: differences over domain 2 between the initial SST (23 March 1998) and (a) the SST field in NCEP reanalysis on 26 March 1998 0000 UT or the SST field simulated on 26 March 1998 0000 UT by (b) ORIGOML, (c) SLABOML, and (d) COMPOML.

during 60 h (Figure 6). The mistral blows over the Gulf of Lions until late in the afternoon on 8 November 1998. The combination of this intense steady mistral and of the strong air-sea thermal contrast leads to extreme values of total turbulent heat flux with a maximum value of nearly 1200 W m^{-2} on average over the MIS domain (Figure 7). The persistence of these strong air-sea exchanges is also highlighted in Figure 7 with a total heat flux that exceeds 500 W m^{-2} on average between 1800 UT on 6 November 1999 and the end of the simulation.

[23] The WRF reference experiments produce realistic simulations of the two studied mistral events, with however slight underestimation of the low-level winds compared to the observations (around 2 m s^{-1} difference on average) [*Flamant*, 2003; *Guénard et al.*, 2006; *Salameh et al.*, 2007]. In the following, the ocean slab schemes performances will be evaluated by quantifying the differences with these reference experiments.

3.2. Ocean Mixed Layer Evolution

3.2.1. Mixed Layer Depth and Current

[24] The OML depth and current are prognostic variables of the slab scheme in ORIGOML and COMPOML. Initially, the OML depth is 50 m over the whole sea domain.

[25] For the mis1 case: after 72 h, the OML has gradually deepened (Figure 8). The deepening is more pronounced in strong wind areas in the two simulations. The maximum deepening is located near Corsica and Sardinia with nearly 55 m depth on 26 March 1998 at 0000 UT. The currents are also quite similar between ORIGOML and COMPOML.

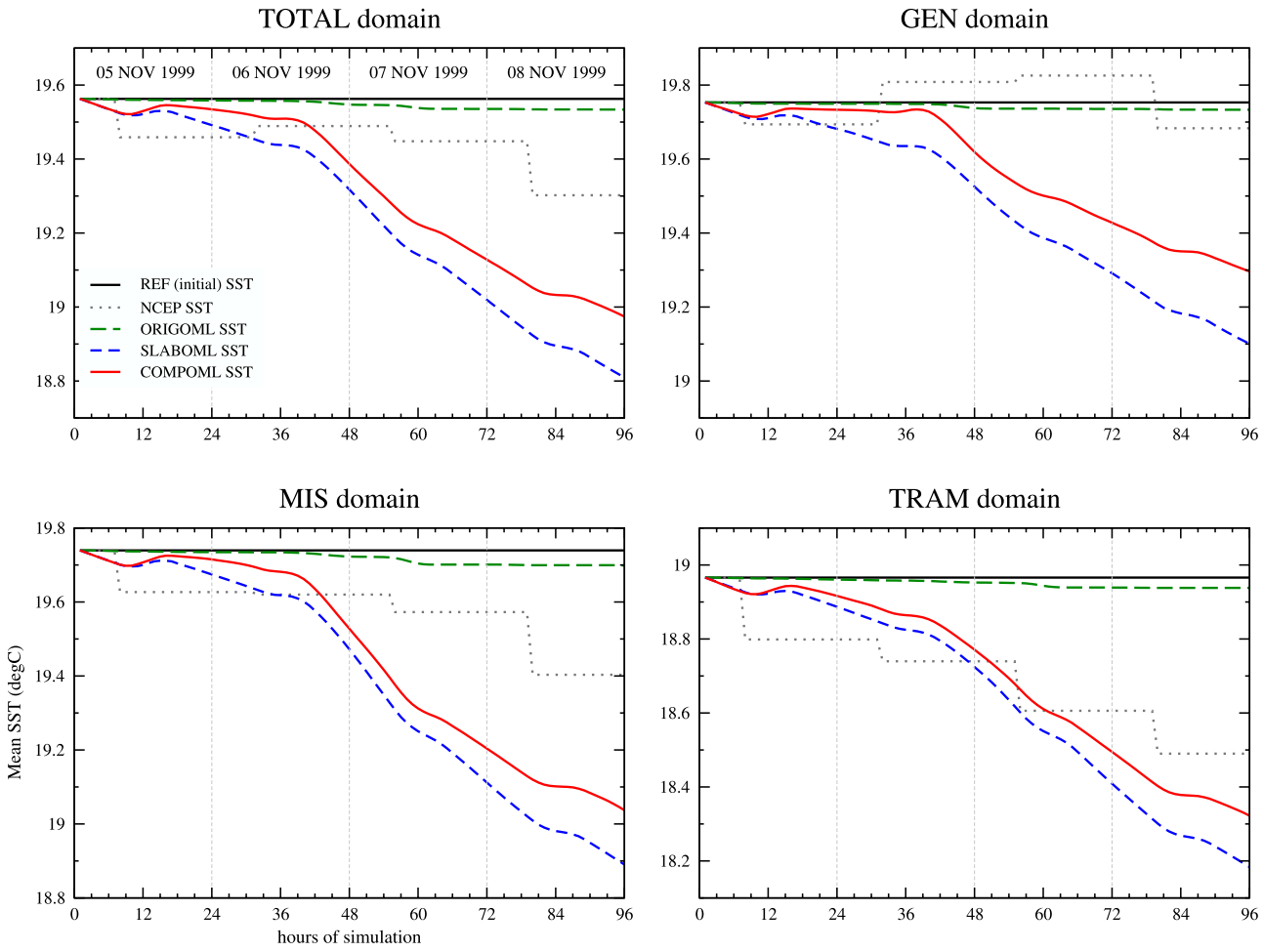

Figure 12. Temporal evolution of the mean SST (°C) during the mis2 case simulations over the TOTAL Sea domain and the GEN, MIS, and TRAM sea domains. Note that the time range is not the same as for mis1 case in Figure 10.

Strong current areas are evidenced East of Corsica and Sardinia and below the tramontane jet (Figure 8). The maximum current is 16 cm s^{-1} in both ORIGOML and COMPOML.

[26] For the mis2 case: after 96 h, the OML has significantly deepened (Figure 9) especially in COMPOML experiment. The deepening is most significant under the strongest and stationary winds, i.e., under mistral and tramontane low-level winds. The maximum deepening is located in the center of domain 2 and reaches nearly 65 m depth on 9 November 1999 at 0000 UT. If the OML deepening is weaker in ORIGOML (52 m on average over the sea domain against 53.5 m in COMPOML on 9 November), the currents are quite similar between ORIGOML and COMPOML experiments (less then 2 cm s^{-1} difference; Figure 9). The strongest currents found are in the Gulf of Lions at 45° to the right of the low-level winds according to the Ekman theory and exceed 35 cm s^{-1} in both ORIGOML and COMPOML.

[27] The differences between the OML responses under the two mistral events can be explained by the stationarity of the wind. The more stationary the intense low-level jet, the larger the energy extraction from the ocean and the deeper the OML. The role of the steadiness of the atmospheric circulation on the intensity of the oceanic response was already highlighted under heavy precipitation events with an onshore low-level jet over the same area [*Lebeaupin et al.*, 2006; *Lebeaupin Brossier et al.*, 2008, 2009] and in the case of tropical cyclones [*Schade and Emanuel*, 1999].

3.2.2. Sea Surface Temperature

[28] For the mis1 case, the NCEP reanalysis captures a gradual SST cooling between 23 and 26 March, particularly in the Gulf of Lions. Averaging over domain 2, the cooling reaches −0.2°C (Figure 10). Maximum cooling of −0.3°C is located to the east of the Rhône river mouth (Figure 11a) and extends 300 km southward. For the mis2 case, the NCEP reanalysis captures a SST cooling on average of −0.25°C (Figure 12). Cooling occurs in the western part of the domain (MIS and TRAM domains, Figure 12), whereas the SST increases in the eastern part (Figure 13a). For the two cases, the NCEP reanalyses capture the SST cooling at different locations, extending over large areas owing to the coarse resolution of the reanalyses.

[29] Small differences in the SST fields are found between the ORIGOML simulation and the reference (Figures 10, 11b, 12, and 13b). For the mis1 case, the cooling reaches only −0.01°C on average over domain 2 after 72 h (Figure 10). For the mis2 case, only a small area is

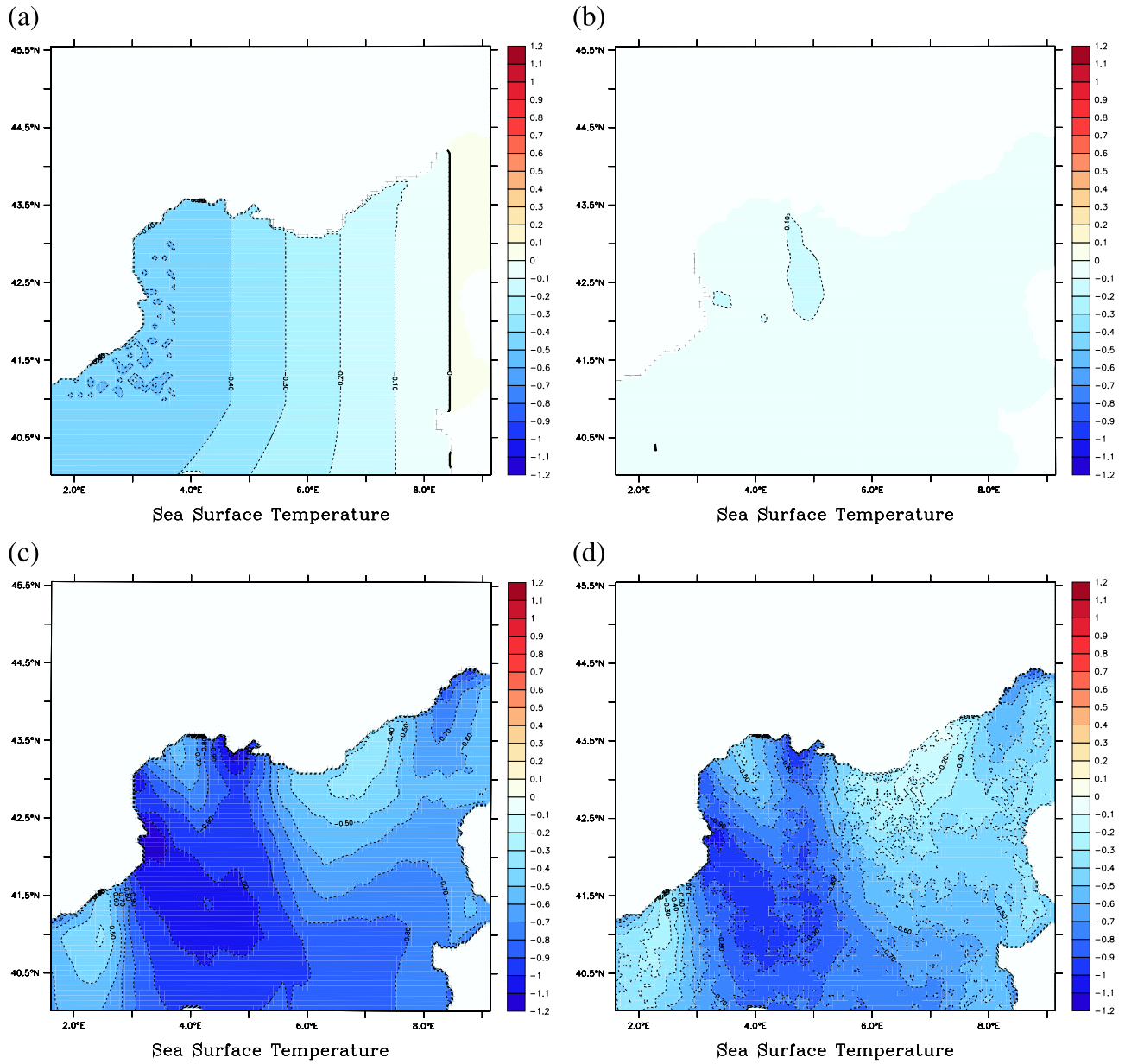

Figure 13. The mis2 case: differences over domain 2 between the initial SST (5 November 1999) and (a) the SST field in NCEP reanalysis the 9 November 1999 0000 UT or the SST field simulated on 9 November 1999 0000 UT by (b) ORIGOML, (c) SLABOML, and (d) COMPOML.

affected by SST cooling reaching −0.1°C on 7 November 1999 when using the ORIGOML slab model (Figure 13b). The contributions of entrainment and transport to the heat budget are thus weak in these two situations. The strongest low-level winds (≃20 m s^{-1}) are not strong enough or stationary enough to induce neither strong h variations nor strong Ekman transport, and consequently variations of the OML temperature are small. This scheme that seems to be adapted to tropical cyclone wind regimes (>30 m s^{-1}) [*Schade and Emanuel*, 1999; *Emanuel et al.*, 2004; Davis and Holland, presented paper, 2007] fails in less severe weather situations, because the contribution of the thermal exchanges at the air-sea interface is missing in this slab model. We thus test slab models accounting for thermal exchanges.

[30] The surface heat fluxes (Figures 5 and 7) induce large SST cooling as evidenced by the SLABOML simulation (Figures 10, 11c, 12, and 13c). For the mis1 case, the net surface heat flux (Q) induces strong SST cooling over the Gulf of Lions, with values similar to those seen in the NCEP reanalysis (Figure 10) over different locations (Figures 11a and 11c). Indeed, the most significant cooling (−0.5°C) is obtained in the eastern part of domain 2, around Corsica and Sardinia and the Gulf of Genoa, where the low-level winds are the strongest and the most persistent. Three SST anomalies are found collocated with the three strong low-level wind flows (tramontane, mistral and Ligurian outflow). At the Rhône river mouth, a −0.1°C cooling after 72 h is induced by the mistral on 24 March. The low-level wind underestimation in the atmospheric simulation limits the SST cooling. The

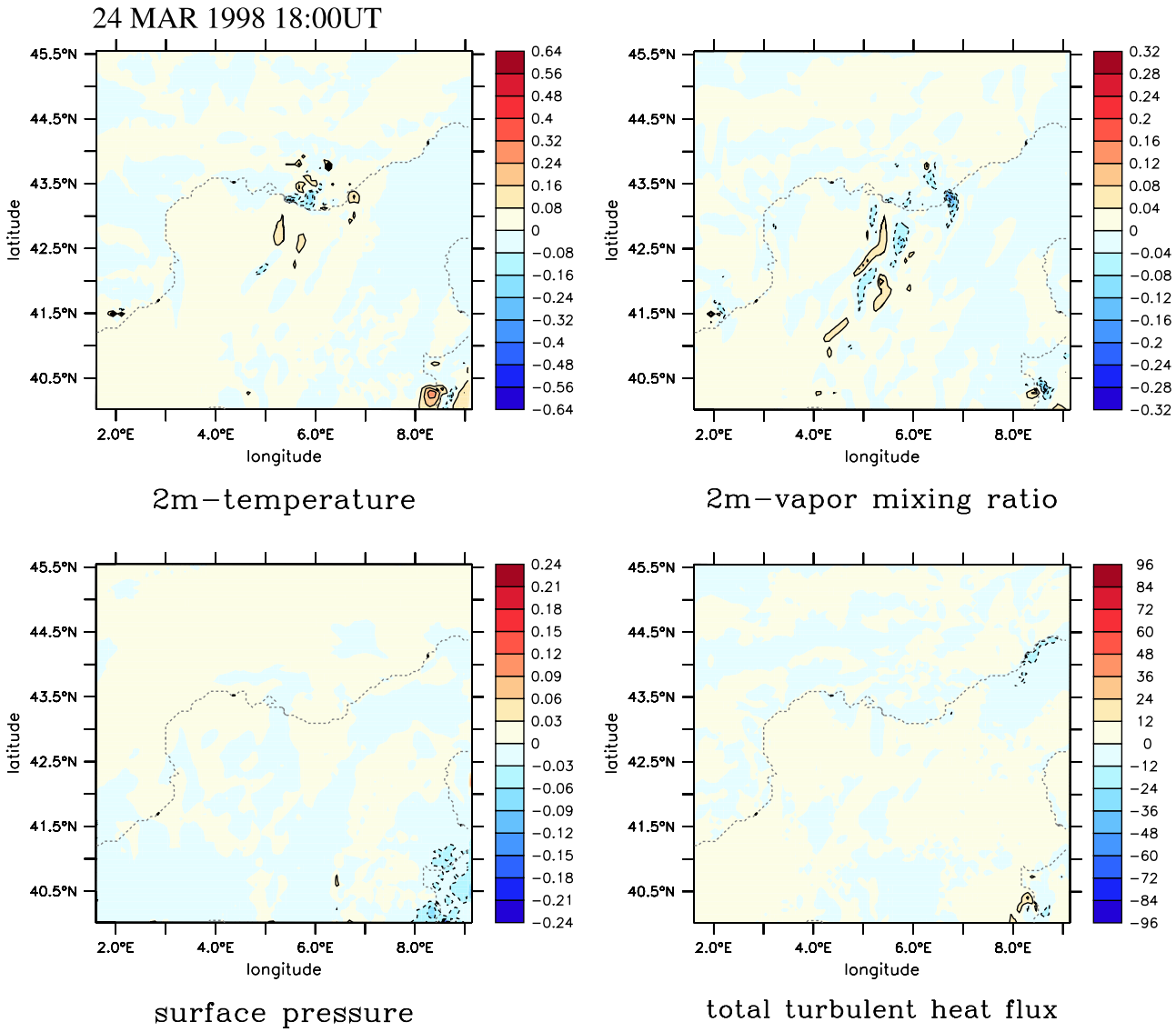

Figure 14. Differences between the COMPOML simulation and the reference experiment (COMPOML-REF) on 24 March 1998 1800 UT for 2-m temperature (°C), 2-m water vapor mixing ratio (g/kg), surface pressure (hPa), and total turbulent sea surface heat flux (H + LE − W m^{-2}) over domain 2.

same results are found for the mis2 case. The slab scheme also produces fine-scale patterns in the SST field correlated with the wind pattern. The strongest SST anomalies reaching −1°C at the end of the simulation are located over the TRAM and MIS subdomains (Figure 12). After 96 h, the SST field shows large cooling below the mistral and tramontane. The SST decrease reaches −1.2°C (Figure 13c). Comparing the SLABOML and ORIGOML simulations shows that the cooling by the sea surface heat fluxes represents more than 90% of the total heat loss against less than 10% due to entrainment.

[31] In COMPOML, we finally obtain SST values ranging between ORIGOML and SLABOML SST values. The COMPOML SST is slightly cooled on average over domain 2 during the mis1 case (Figure 10). The final SST field exhibits a strong cooling of −0.45°C in the Gulf of Genoa (Figure 11d), but also a SST warming where the low-level winds are weaker. Figure 10 shows that SLABOML and COMPOML simulations predict quite similar SST trends (-2.5×10^{-3}°C h^{-1} in SLABOML and -1.8×10^{-3}°C h^{-1} in COMPOML). The difference between the two curves (Figure 10) is due to the gradual OML deepening in the COMPOML simulation. In fact, at the beginning the same energy (Q) is extracted from the OML in the two simulations, the deepening ($h > h_0$) in COMPOML tends to limit the SST cooling, and in turns gradually induces stronger net heat flux in COMPOML than in SLABOML. For the mis2 case, the SST field shows large cooling after 96 h below the mistral and tramontane reaching −1.1°C (Figure 13d). When using the complete equation system (COMPOML experiments), the gradual OML deepening limits the temperature decrease even if the same amount of heat is exchanged at the air-sea interface than in SLABOML. As evidenced by equation (7), $\frac{\partial T}{\partial t}$ scales as h^{-1} and thus decreases as h increases. It

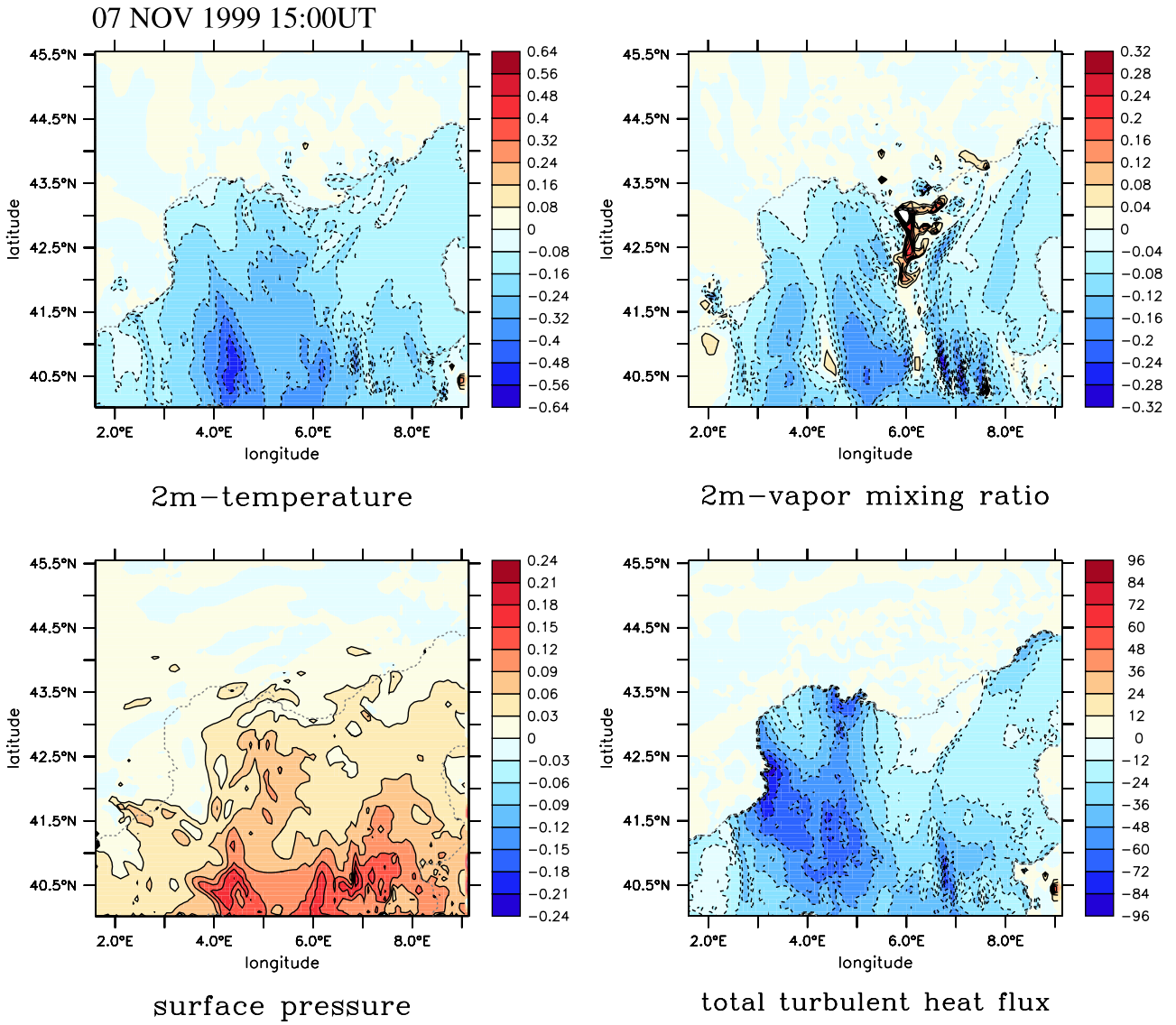

Figure 15. As in Figure 14 but for 7 November 1999 1500 UT.

gradually induces a stronger net heat flux in COMPOML than in SLABOML (Figure 7) that finally enhances the difference between the two SST evolution curves. The temporal averaged SST trends are -7.8×10^{-3}°C h^{-1} in SLABOML and -6.1×10^{-3}°C h^{-1} in COMPOML for the mis2 case (Figure 12).

[32] The difference of the stationarity of the strong winds between the two mistral events studied here explain the difference in the OML temperature trends. The SLABOML and COMPOML experiments show that the intensity and the persistence of the turbulent heat fluxes are the controlling factors for the OML temperature. Indeed, the stationarity of the strong low-level winds and an intense thermal contrast between the OML and the ABL in the mis2 case combine to produce intense sensible and latent heat fluxes, and consequently result in a significant energy amount extracted from the OML toward the ABL. For the mis1 case a smaller thermal contrast and weaker low-level winds produce 4 times less heat flux values (Figures 5 and 7) and consequently less significant SST trends. In the sheltered regions in the lee of the Alps and Massif Central, the OML temperature variations are more sensitive to the radiative fluxes. As the turbulent fluxes are less significant in these areas, the OML deepening and the currents are also weak.

3.3. Feedbacks on the Atmospheric Simulations

[33] We focus here on differences obtained for the atmospheric low-level fields (temperature and humidity at 2 m, surface pressure, total turbulent heat flux and the 10-m wind) between the reference and the SLABOML and COMPOML simulations which evidence the most significant oceanic response.

[34] Indeed, as the SST slowly decreases in COMPOML (and SLABOML) simulation, the sensible and latent heat fluxes also decrease (Figures 5 and 7). A smaller heat amount (-25 W m^{-2} and -100 W m^{-2} locally in COMPOML (and SLABOML) for the mis1 and mis2 cases, respectively) is transported across the air-sea interface to the atmospheric boundary layer, leading to colder low-level air and conse-

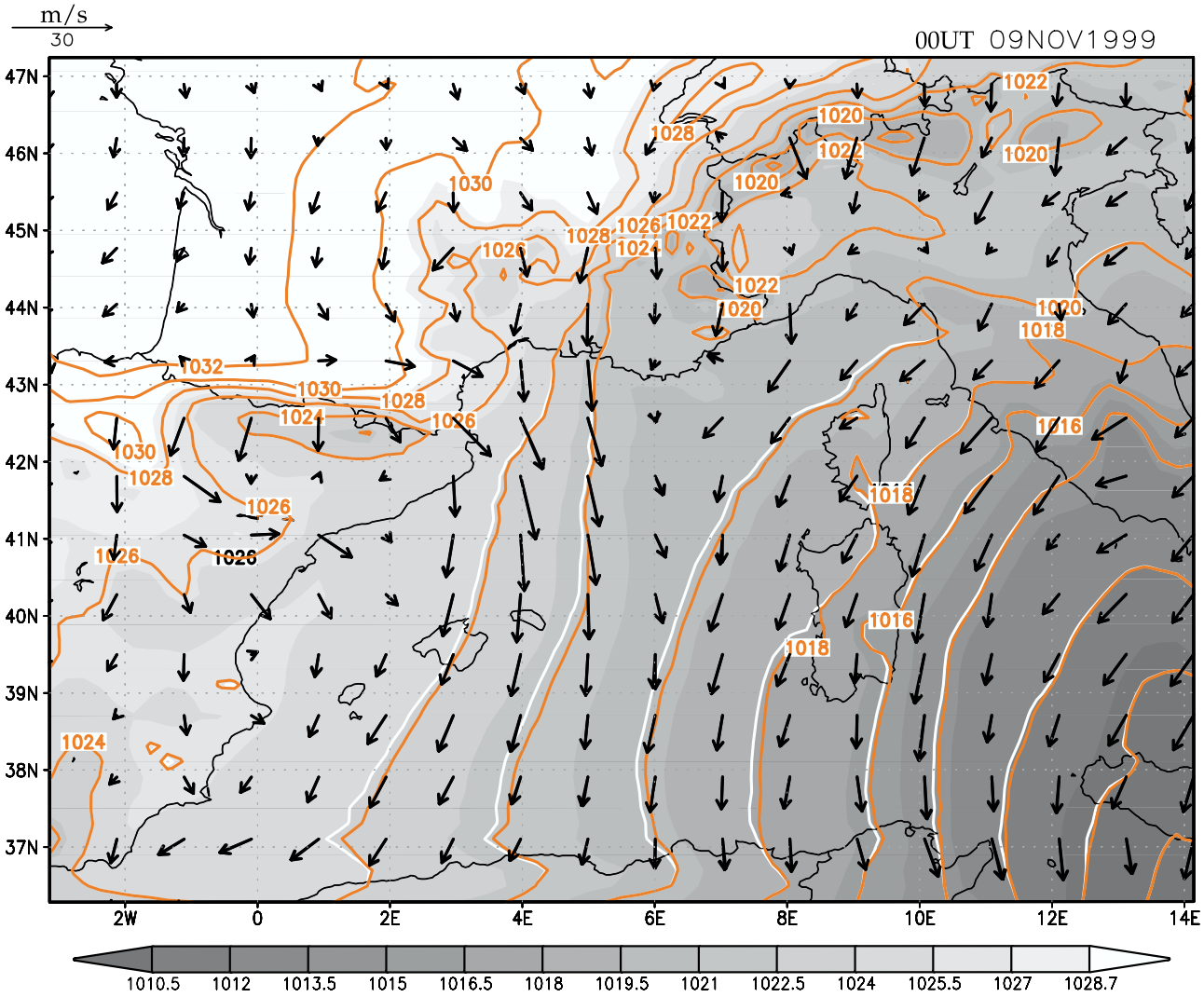

Figure 16. For 9 November 1999 at 0000 UT over domain 1: sea level pressure (SLP in hPa, greyscale and white isocontours) and 10-m wind (m s^{-1}, arrows) simulated by the reference experiment and SLP simulated by SLABOML (red isocontours).

quently to a more stable air mass than in the reference experiment (Figures 14 and 15). Less significant responses are found for humidity, pressure and wind fields. The low-level air mass is more stable in SLABOML and COMPOML with a slightly larger surface pressure.

[35] Changing the ocean surface scheme induces minor modifications of the trough location and intensity: it is however visible for the mis2 case as shown in Figure 16. Such modifications do not appear for the mis1 case simulations. These differences in the low-level trough position induce modification in the low-level wind direction in the Gulf of Lions. In fact, the most significant surface wind modifications are located in the wake of the Alps, where winds are weak for the two situations (Figures 17 and 18). This modifications correspond to a shift of the mistral to the east in COMPOML (and SLABOML) compared to the reference experiment (Figure 18). This area finally shows the strongest sensitivity to SST variations. *Flamant* [2003] already highlighted the significant impact of these sheltered regions positions which evolve with the synoptic conditions on the local sea surface turbulent fluxes.

[36] In ORIGOML, the air temperature response is less significant than in SLABOML and COMPOML, but differences in the wind field are still present in the wake area. The SST evolution impact on the dynamics at low levels in the weak regime should imply several nonlinear interactions between the two boundary layers affecting the very local scale. A small signature in the potential vorticity field has been seen when ORIGOML is compared to the reference (not shown).

[37] The coupled numerical experiments evidence feedbacks between the interactive OML and ABL dynamics. The coupling tends to gradually decrease the thermal gradient between the OML and the ABL. The low-level atmospheric temperature and humidity fields are the most sensitive to the heat fluxes decrease. In fact, the SST decrease tends to stabilize the low level air mass. An interactive OML does not change the upper-level dynamics. Only a small modification of the low-level trough has been found for the mis2

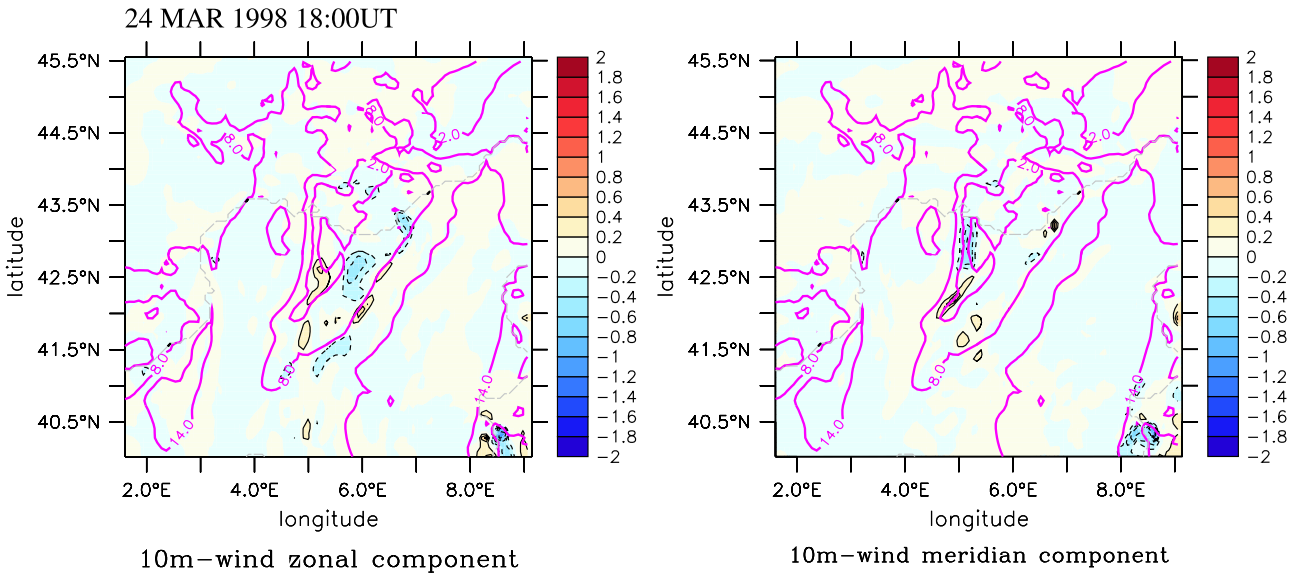

Figure 17. Differences between the COMPOML simulation and the reference experiment (COMPOML-REF) on 24 March 1998 1800 UT for the 10-m wind components over domain 2. Purple thick lines delineate 10-m wind speed module values in the REF simulation (m s^{-1}).

case. This faster eastward progression of the trough leads to an eastward shift of the mistral direction over the Gulf of Lions more particularly in the sheltered areas.

4. Conclusion

[38] Coupling the high-resolution atmospheric model WRF to a slab ocean model shows a strong cooling of the ocean mixed layer during the tramontane/mistral events of 23–26 March 1998 (mis1) and of 5–9 November 1999 (mis2). With these two mistral situations, we highlighted that the modeled ocean response is sensitive to the strength of the low-levels winds but also to their persistence and to the thermal contrast between the ocean and the atmosphere. The short mistral duration and the relatively cold OML in March 1998 (after the winter) in the mis1 case produce moderate turbulent heat fluxes over a short period. The energy amount extracted toward the air-sea interface is not strong enough to perturb the OML thermodynamics. Conversely, during the mis2 case, the long duration of high winds with a significant air-sea thermal contrast (as the SST is still relatively warm in November) produce intense heat exchanges (>500 W m^{-2} during 60 h). In this situation, the full ocean slab model, which includes surface the heat and momentum fluxes, the Coriolis force, the entrainment and the Ekman transport, produces an OML cooling and deepening. Our sensitivity experiments show that taking the surface net heat budget into account is preferable to correctly

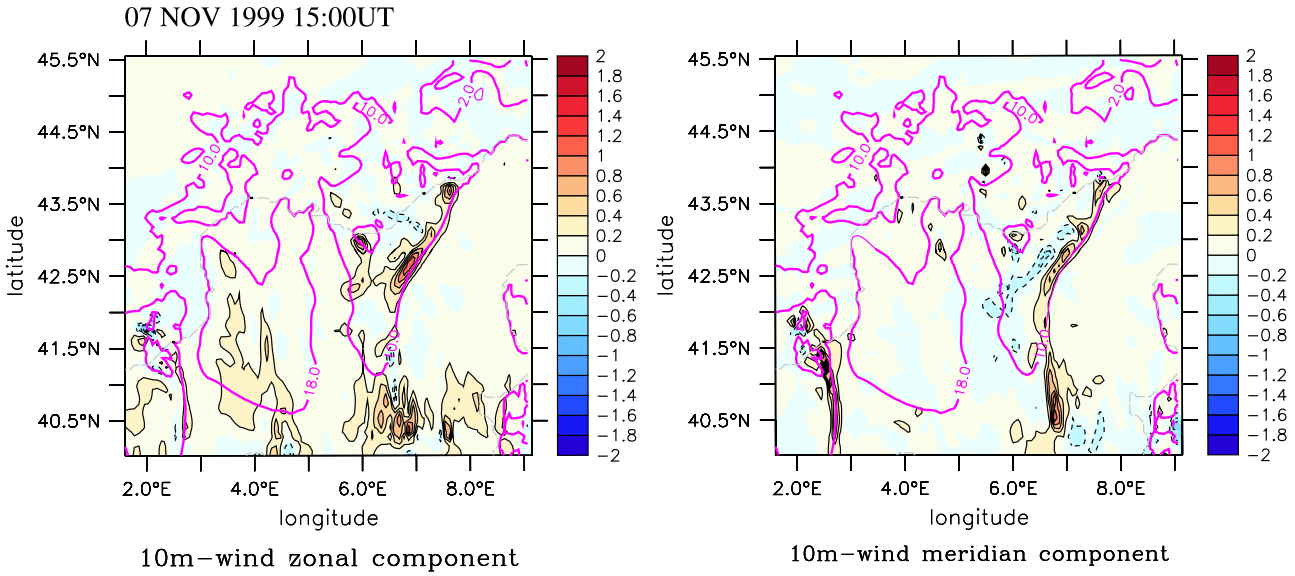

Figure 18. As in Figure 17 but for 7 November 1999 1500 UT.

estimate the OML response under these severe winds events instead of the original scheme only driven by the wind stress. Small feedbacks on the atmospheric event have been seen: the coupling tends to decrease the gradients between air and sea at the interface and modulates temperature contrasts. The low-level atmospheric temperature and humidity fields are modified according to the air-sea turbulent heat fluxes decrease. The dynamics are finally slightly changed by taking into account an interactive OML. A small modification of the trough has been found leading to a weak modification of the low-level wind direction over the Gulf of Lions and of the horizontal extensions of the sheltered areas.

[39] Note that slab schemes strongly depend on parameters values (h_0 and eventually γ). Other choices for these parameters values could lead to different results. In particular, a shallower OML could lead to more significant SST cooling under the same atmospheric event, whereas a deeper OML would require more energy extraction to simulate the same oceanic response. In particular, the deepening simulated in COMPOML leads to a less intense SST decrease than in SLABOML for this main reason.

[40] The results obtained in our experiments show a production of fine scale oceanic patterns under strong mistral events that could not be reproduced in large-scale analyses. The produced patterns look like the fine-scale structures that could be found in high-resolution satellite products like AVHRR SST fields [*Estournel et al.*, 2003; *Lebeaupin et al.*, 2006]. Nevertheless, without mesoscale assimilation of oceanic data, our SST field cannot be directly compared quantitatively to the AVHRR SST fields. At first order, as the ocean schemes are initialized with the NCEP reanalyses, the SST keeps the main structure of the coarse initial field. A more thorough insight shows that the strong anomalies of the SST field simulated during mis2 case probably persisted several days over the Gulf of Lions, as evidenced by the cold anomaly found in the AVHRR SST field used by *Lebeaupin et al.* [2006] study of the 12 November 1999 heavy precipitation event (Aude case), whereas this anomaly is not present in the coarse SST field of the NCEP analyses.

[41] Even if the atmospheric simulation is not very sensitive to the gradual SST evolution during the two studied mistral events here, an accurate SST initial field at fine scale is crucial to succeed in reproducing the air-sea heat exchanges during a sequence of several high wind events over a small region as the Gulf of Lions. This highlights the pertinence of coupling a slab ocean model including entrainment, advection and surface exchange processes to a weather forecasting model to better catch the OML evolution a few days before and during severe weather events and finally obtain a better SST analysis even when satellite data are missing in cloudy conditions. The complete slab ocean scheme is a robust and cheap numerical tool that allows an estimation of the fine-scale SST evolution within the WRF model.

[42] A high-resolution two-way coupling with a tridimensional ocean model is now needed for estimating the ocean state modifications under a succession of strong mistral events during the winter ocean deep convection preconditioning phase in the Gulf of Lions and for studying the formation of local gyres and coastal upwellings under strong tramontane/mistral. Validation of slab oceanic models as well as the fully coupled model is also expected from the HyMeX experiment(HYdrological cycle in Mediterranean EXperiment, http://www.cnrm.meteo.fr/hymex/) that aims to study the full hydrological cycle over the Mediterranean basin and in particular the intense air-sea exchanges occurring under severe meteorological situations.

[43] **Acknowledgments.** This work is a contribution to the MORCE-MED project funded by the GIS (Groupement d'Intérêt Scientifique) "Climat, Environnement et Société" (http://www.gisclimat.fr/Doc/GB/D_projects/MORCE_MED_GB.html). The authors are grateful to the "wrfhelp" team, and to Sophie Bastin, Dmitry Khvorostiyanov, and Julien Lenseigne, for their useful advice and help about the use of the WRF numerical model. The authors finally thank Tamara Salameh, Karine Béranger, and Hervé Giordani for fruitful discussions about this work.

References

Bastin, S., P. Drobinski, V. Guénard, J.-L. Caccia, B. Campistron, A. M. Dabas, P. Delville, O. Reitebuch, and C. Werner (2006), On the interaction between sea breeze and summer mistral at the exit of the Rhône Valley, *Mon. Weather Rev.*, *134*, 1647–1668.

Bender, M. A., I. Ginis, and Y. Kurihara (1993), Numerical simulations of tropical cyclone-ocean interaction with a high-resolution coupled model, *J. Geophys. Res.*, *98*(D12), 23,245–23,263.

Drévillon, M., C. Cassou, and L. Terray (2003), Model study of the North Atlantic region atmospheric response to autumn tropical Atlantic sea-surface-temperature anomalies, *Q. J. R. Meteorol. Soc.*, *129*, 2591–2611.

Drobinski, P., S. Bastin, V. Guénard, J.-L. Caccia, A. M. Dabas, P. Delville, A. Protat, O. Reitebuch, and C. Werner (2005), Summer mistral at the exit of the Rhône valley, *Q. J. R. Meteorol. Soc.*, *131*, 353–375.

Dudhia, J. (1989), Numerical study of convection observed during the winter monsoon experiment using a mesoscale two-dimensional model, *J. Atmos. Sci.*, *46*, 3077–3107.

Ekman, V. W. (1905), On the influence of the Earth's rotation on ocean currents, *Arch. Math. Astron. Phys.*, *2*, 1–53.

Emanuel, K., C. DesAutels, C. Holloway, and R. Korty (2004), Environmental control of tropical cyclone intensity, *J. Atmos. Sci.*, *61*, 843–858.

Estournel, C., X. Durrieu de Madron, P. Marsaleix, F. Auclair, C. Julliand, and R. Vehil (2003), Observation and modeling of the winter coastal oceanic circulation in the Gulf of Lion under wind conditions influenced by the continental orography (FETCH experiment), *J. Geophys. Res.*, *108*(C3), 8059, doi:10.1029/2001JC000825.

Flamant, C. (2003), Alpine lee cyclogenesis influence on air-sea heat exchanges and marine atmospheric boundary layer thermodynamics over the western Mediterranean during a Tramontane/Mistral event, *J. Geophys. Res.*, *108*(C2), 8057, doi:10.1029/2001JC001040.

Gal-Chen, T., and R. C. J. Sommerville (1975), On the use of a coordinate transformation for the solution of the Navier-Stokes equations, *J. Comput. Phys.*, *17*, 209–228.

Gaspar, P. (1988), Modelling of seasonal cycle of the upper ocean, *J. Phys. Oceanogr.*, *18*, 161–180.

Guénard, V., P. Drobinski, J. L. Caccia, G. Tedeschi, and P. Currier (2006), Dynamics of the MAP IOP 15 severe Mistral event: Observations and high-resolution numerical simulations, *Q. J. R. Meteorol. Soc.*, *32*, 757–777.

Hong, S. Y., J. Dudhia, and S.-H. Chen (2004), A revised approach to ice microphysical processes for the bulk parameterization of clouds and precipitation, *Mon. Weather Rev.*, *132*, 103–120.

Kain, J. S. (2004), The Kain-Fritsch convective parameterization: An update, *J. Appl. Meteorol.*, *43*, 170–181.

Kalnay, E., et al. (1996), The NCEP/NCAR 40-Year Reanalysis Project, *Bull. Am. Meteorol. Soc.*, *77*(3), 437–471.

Kara, A. B., A. J. Wallcraft, P. J. Martin, and E. P. Chassignet (2008), Performance of mixed layer models in simulating SST in the equatorial Pacific Ocean, *J. Geophys. Res.*, *113*, C02020, doi:10.1029/2007JC004250.

Lau, N.-C., and M. J. Nath (2006), ENSO modulation of the interannual and intraseasonal variability of the East Asian monsoon—A model study, *J. Clim.*, *19*(18), 4508–4530, doi:10.1175/JCLI3878.1.

Lebeaupin, C., V. Ducrocq, and H. Giordani (2006), Sensitivity of Mediterranean torrential rain events to the sea surface temperature based on high-resolution numerical forecasts, *J. Geophys. Res.*, *111*, D12110, doi:10.1029/2005JD006541.

Lebeaupin Brossier, C., V. Ducrocq, and H. Giordani (2008), Sensitivity of three Mediterranean heavy rain events to two different sea surface fluxes parameterizations in high-resolution numerical modeling, *J. Geophys. Res.*, *113*, D21109, doi:10.1029/2007JD009613.

Lebeaupin Brossier, C., V. Ducrocq, and H. Giordani (2009), Two-way one-dimensional high-resolution air-sea coupled modelling applied to Mediterranean heavy rain events, *Q. J. R. Meteorol. Soc.*, *135*, 187–204.

Li, L., A. Bozec, S. Somot, K. Béranger, P. Bouruet-Aubertot, F. Sevault, and M. Crépon (2006), Regional atmospheric, marine processes and climate modelling, in *Mediterranean Climate Variability and Predictability*, edited by P. Lionello, P. Malanotte-Rizzoli, and R. Boscolo, pp. 373–397, Elsevier, Amsterdam.

Millot, C. (1979), Wind induced upwellings in the Gulf of Lions, *Oceanol. Acta*, *2*, 261–274.

Mlawer, E. J., S. J. Taubnam, P. D. Brown, M. J. Iacono, and S. A. Clough (1997), Radiative transfer for inhomogeneous atmospheres: RRTM, a validated correlated k-model for the longwave, *J. Geophys. Res.*, *102*(D14), 16,663–16,682.

Monin, A. S., and A. M. Obukhov (1954), Basic laws of turbulent mixing in the surface layer of the atmosphere, *Contrib. Geophys. Inst. Acad. Sci. USSR*, *151*, 163–187.

Noh, Y., W. G. Cheon, S.-Y. Hong, and S. Raasch (2003), Improvement of the K-profile model for the planetary boundary layer based on large eddy simulation data, *Boundary Layer Meteorol.*, *107*, 401–427.

Pollard, R. T., P. B. Rhines, and R. O. R. Y. Thompson (1973), The deepening of the wind-mixed layer, *Geophys. Astrophys. Fluid Dyn.*, *4*(1), 381–404.

Price, J. F. (1981), Upper ocean response to a hurricane, *J. Phys. Oceanogr.*, *11*, 153–175.

Pullen, J., J. D. Doyle, R. Hodur, A. Ogston, J. W. Book, H. Perkins, and R. P. Signell (2003), Coupled ocean-atmosphere nested modeling of the Adriatic Sea during winter and spring 2001, *J. Geophys. Res.*, *108*(C10), 3320, doi:10.1029/2003JC001780.

Pullen, J., J. D. Doyle, and R. P. Signell (2006), Two-way air-sea coupling: A study of the Adriatic, *Mon. Weather Rev.*, *134*, 1465–1483.

Pullen, J., J. D. Doyle, T. Haack, C. Dorman, R. P. Signell, and C. M. Lee (2007), Bora event variability and the role of air-sea feedback, *J. Geophys. Res.*, *112*, C03S18, doi:10.1029/2006JC003726.

Salameh, T., P. Drobinski, L. Menut, B. Bessagnet, C. Flamant, A. Hodzic, and R. Vautard (2007), Aerosol distribtion over the western Mediterranean basin during a Tramontane/Mistral event, *Ann. Geophys.*, *25*, 2271–2291.

Schade, L. R., and K. A. Emanuel (1999), The ocean's effect on the intensity of tropical cyclones: Results from a simple coupled atmosphere-ocean model, *J. Atmos. Sci.*, *56*, 642–651.

Skamarock, W. C., J. B. Klemp, J. Dudhia, D. O. Gill, D. M. Barker, M. G. Duda, X.-Y. Huang, W. Wang, and J. G. Powers (2008), A description of the Advanced Research WRF Version 3, *NCAR Tech. Note NCAR/TN-475+STR*, 125 pp., Natl. Cent. for Atmos. Res., Boulder, Colo.

Smith, T. M., and R. Reynolds (2003), Extended reconstruction of global sea surface temperatures based on COADS data (1854–1997), *J. Clim.*, *16*, 1495–1510.

P. Drobinski and C. Lebeaupin Brossier, LMD, IPSL, Ecole Polytechnique, Plateau de Palaiseau, Route de Saclay, F-91128 Palaiseau CEDEX, France. (cindy.lebeaupin@lmd.polytechnique.fr)